SANDIA REPORT
SAND2016-11187
Unlimited Release
Printed November 2016

Applying the World Water and Agriculture Model to Filling Scenarios for the Grand Ethiopian Renaissance Dam

Daniel L. Villa, Vincent C. Tidwell, Howard D. Passell, and Barry L. Roberts

Prepared by
Sandia National Laboratories
Albuquerque, New Mexico 87185 and Livermore, California 94550

Sandia National Laboratories is a multi-mission laboratory managed and operated by Sandia Corporation, a wholly owned subsidiary of Lockheed Martin Corporation, for the U.S. Department of Energy's National Nuclear Security Administration under contract DE-AC04-94AL85000.

Issued by Sandia National Laboratories, operated for the United States Department of Energy by Sandia Corporation.

Available to DOE and DOE contractors from
U.S. Department of Energy
Office of Scientific and Technical Information
P.O. Box 62
Oak Ridge, TN 37831

Telephone: (865) 576-8401
Facsimile: (865) 576-5728
E-Mail: reports@osti.gov
Online ordering: http://www.osti.gov/scitech

Available to the public from
U.S. Department of Commerce
National Technical Information Service
5301 Shawnee Rd
Alexandria, VA 22312

Telephone: (800) 553-6847
Facsimile: (703) 605-6900
E-Mail: orders@ntis.gov
Online order: http://www.ntis.gov/search

SAND2016-11187
Unlimited Release
Printed November 2016

Applying the World Water and Agriculture Model to Filling Scenarios for the Grand Ethiopian Renaissance Dam

Daniel Villa
Earth Systems Analysis

Vincent C. Tidwell
Earth Systems Analysis

Howard D. Passell
Policy and Decision Analytics

Barry L. Roberts
Geotechnology and Engineering

Sandia National Laboratories
P.O. Box 5800
Albuquerque, New Mexico 87185-MS1138

Abstract

The World Water and Agriculture Model has been used to simulate water, hydropower, and food sector effects in Egypt, Sudan, and Ethiopia during the filling of the Grand Ethiopian Renaissance Dam reservoir. This unique capability allows tradeoffs to be made between filling policies for the Grand Ethiopian Renaissance Dam reservoir. This Nile River Basin study is presented to illustrate the capacity to use the World Water and Agriculture Model to simulate regional food security issues while keeping a global perspective. The study uses runoff data from the Intergovernmental Panel for Climate Change Coupled Model Inter-comparison Project Phase 5 and information from the literature in order to establish a reasonable set of hydrological initial conditions. Gross Domestic Product and population growth are modelled exogenously based on a composite projection of United Nations and World Bank data. The effects of the Grand Ethiopian Renaissance Dam under various percentages of water withheld are presented.

ACKNOWLEDGEMENTS

The authors of this SAND Report, “Applying the World Water and Agriculture Model to Filling Scenarios of the Grand Ethiopian Renaissance Dam,” would like to acknowledge and give a special thanks to Ximing Cai for providing the modeling framework to create the World Water and Agriculture Model on which this study is based.

CONTENTS

FIGURES

TABLES

ACRONYMS

AR	Assessment Report
BIA	Behavioral Influence Assessment
CIESIN	Center for International Earth Science Information Network
CMIP5	Coupled Model Inter-comparison Project Phase 5
FAO	Food and Agriculture Organization
FPU	Food Production Units
GCM	General Circulation Model
GDP	Gross Domestic Product
GERD	Grand Ethiopian Renaissance Dam
GFDL	Geophysical Fluid Dynamics Laboratory
GRDC	Global Runoff Data Center
IFPRI	International Food Policy Research Institute
IMPACT	International Model for Policy Analysis of Commodities and Trade
IPCC	Intergovernmental Panel for Climate Change
IWMI	International Water Management Institute
LTA	Long Term Average
RCP	Representative Concentration Pathways
UN	United Nations
WSM	Water Simulation Model
WWAM	World Water and Agriculture Model

NOMENCLATURE

Equation (1)

DA	Total agricultural demand in cubic kilometers for all crops
AI	Irrigated area calculated by IMPACT in million hectares (10^{10} meters squared)
ETP	Long term average potential evapotranspiration of the current crop and month in millimeters
PEF	Long term average effective precipitation in millimeters
EE	Effective efficiency for the current crop and FPU
RWP	Relative price of water
ϵ	Price elasticity for the *RWP*
$\otimes$	Operator indicates an element-wise multiplication of the matrices for shared indices which are not being summed
c index	Crops which include the crop type commodities
u index	Set of 282 FPUs
m index	Represents the month
y index	Stands for the range of years simulated

Equation (2)

DL	Actual demand for livestock by year, month, and FPU
AL	Total mass of livestock from IMPACT for a given year, FPU, and livestock type
WU	Water use per livestock given livestock type and FPU
dl	Vector with 12 elements which sums to 1
y index	Stands for the range of years simulated
m index	Represents the month
u index	Set of 282 FPUs
a index	Livestock type

Equation (3)

DM	Municipal Demand
DM0	Initial municipal demand
POP I	Population
GDP	gross domestic product
α and β	Demand elasticity constants which have been set to 1 for population and 0.5 for GDP
y index	Stands for the range of years simulated
m index	Represents the month
u index	Set of 282 FPUs
a index	Livestock type

Equations (4) and (5)

CD	Climate data
HR	Historical long term average runoff from Global Runoff Data Center
F_Y	Yearly scaling factor relative to the climate data long term average
u index	Set of 282 FPUs
y index	Set of years 2006-2050
m index	Represents the month
FR_{umy}	Desired future runoff scenario

Equations (6) (7) (8) (9) and (10)

E	Elevation in meters
A	*Lake surface area*
V	*Volume of water*

Equations (11) and (12)

P	Average power output over a month of time in megawatts
Q	Discharge through the turbines in millions of cubic meters per month
z	The head in meters
E	*Elevation* in meters

Equations (13) and (14)

η_T	Turbine efficiency
ρ	Gravity of water
Q	Release
z	Head in meters
V	*Volume of water*

This Page is Intentionally Left Blank

EXECUTIVE SUMMARY

The World Water and Agriculture Model (WWAM) has been applied to Egypt, Sudan, and Ethiopia during the filling of the Grand Ethiopian Renaissance Dam (GERD) reservoir. WWAM provides a unique capability by providing water, hydropower, and food sector balances as a function of filling policies for the GERD. WWAM needs to be globally calibrated to more recent data before these results can be considered to be accurate with respect to countries outside the Nile River Basin. The preliminary results presented are therefore a capabilities demonstration which has undergone enough scrutiny at the Nile River Basin to produce reasonable results in Egypt.

A two dimensional parameter study of the Nile River Basin Food Production Units (FPUs) which investigated the effects of the GERD and climate was executed using WWAM. The FPUs involved and the geography of the Nile River Basin are shown in Figure 1 and Figure 2. Sixteen filling cases were run which involve withholding 0% to 50% of the Blue Nile River stream flow. These GERD filling scenarios were run across five climate scenarios developed from estimates of future runoff in the Nile River Basin in the literature. The climate scenarios include: long term average (LTA) data from the Global Runoff Data Center (GRDC) and data from the Intergovernmental Panel for Climate Change (IPCC) Coupled Model Inter-comparison Project Phase Five (CMIP5) Representative Concentration Pathways 8.5 (RCP 8.5) climate scenario. The specific results used from CMIP5 came from the geophysical fluid dynamics laboratory (GFDL) model. IPCC CMIP5 GFDL RCP8.5 represents a high emissions future.

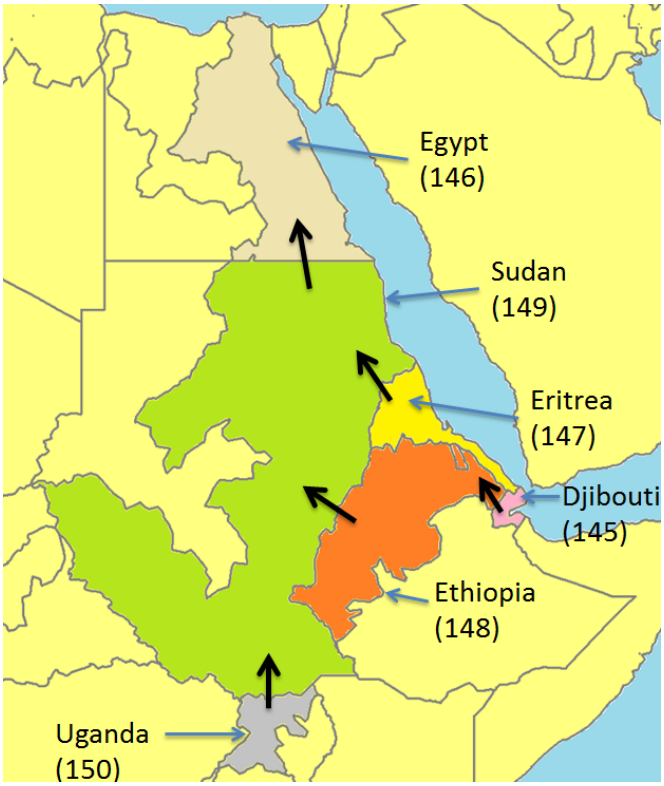

Figure 1. Flow Paths for Nile River Basin FPUs

Source: Printing and Multimedia, General Services Department, the World Bank Group

Figure 2. Detailed Geography of Nile River Basin

Egyptian water storage for all 80 cases is shown in Figure 3 with "no GERD" and "10% water withheld" cases highlighted. This figure shows that population and economic growth are the primary drivers of decreasing water reserves in Egypt but that the GERD causes Egypt to run out of water several years earlier than in its absence. The wide range of water futures being represented should provide strong evidence that Egypt needs to address its future water security through sources other than the Nile River. The GERD is not the determining factor in Egypt running out of water reserves but does quicken the timing and severity of water shortages.

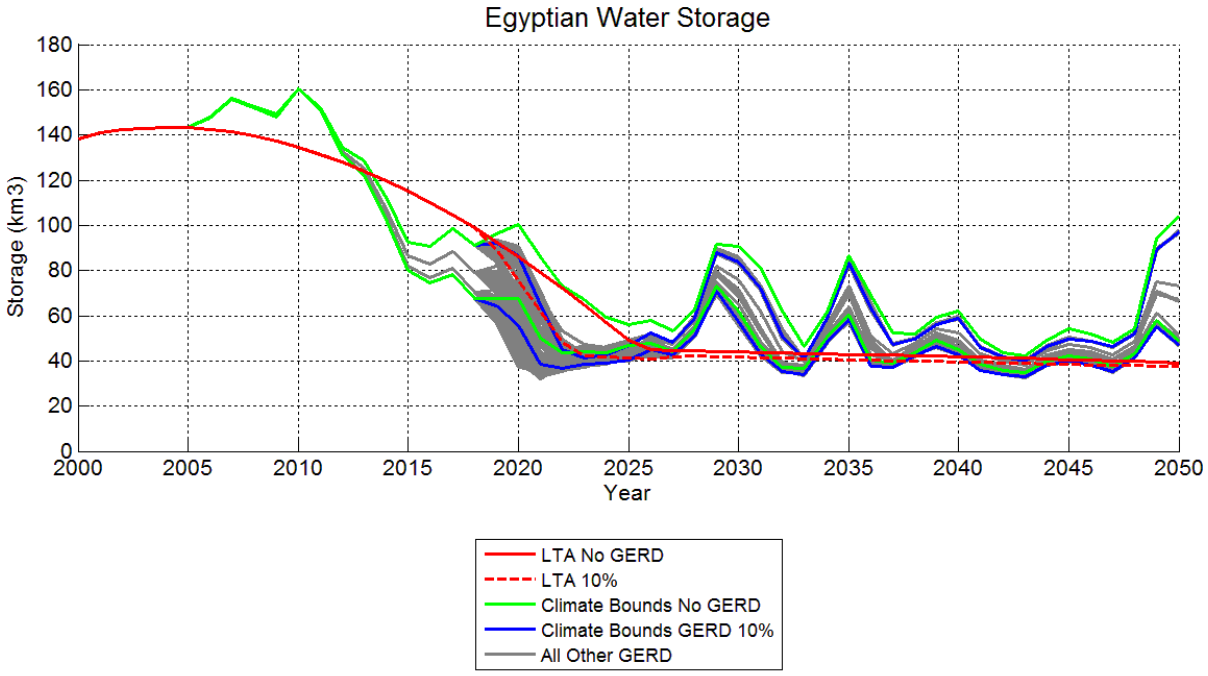

Figure 3. Egyptian Storage Versus Time

Figure 4 shows the same plot for food production. For fast fill rates (25%-50%), a significant shock of as much as a 20% decrease in food production occurs. Such significant drops indicate economic hardship and may drive unrest if food prices also spike. The first set of disruptions from 2018 to 2028, are primarily driven by the GERD in 2018. The other disruptions are due to variations in climate. The GERD will produce more hydropower that may make up for these food production drops. Even so, this result favors filling the GERD more slowly. These conclusions need to be weighed against psychological effects of the GERD on Egyptians and Ethiopians. This addition can be achieved by coupling WWAM results with models such as the Behavioral Influence Assessment (BIA) model developed at Sandia National Laboratories (Backus et. al., 2010, Bernard et. al., 2016).

The current results indicate that there is no clear optimal GERD filling policy with respect to net food production lost. This is the case because climate uncertainty changes the fill rate which minimizes food losses as seen in Figure 5 where LTA and four scaled versions of runoff for the IPCC CMIP5 GFDL RCP 8.5 scenario are shown. Notice that the maximum varies erratically with

fill rate. This variation in optimum leads to the conclusion that the goal of keeping food losses in Egypt to a minimum through GERD policies is not achievable in the face of climate uncertainty. Further runs with more climate realizations might reveal a statistically optimal answer but no clear optimum exists from this study. More flexible policies than withholding a constant percentage of flow should therefore be investigated.

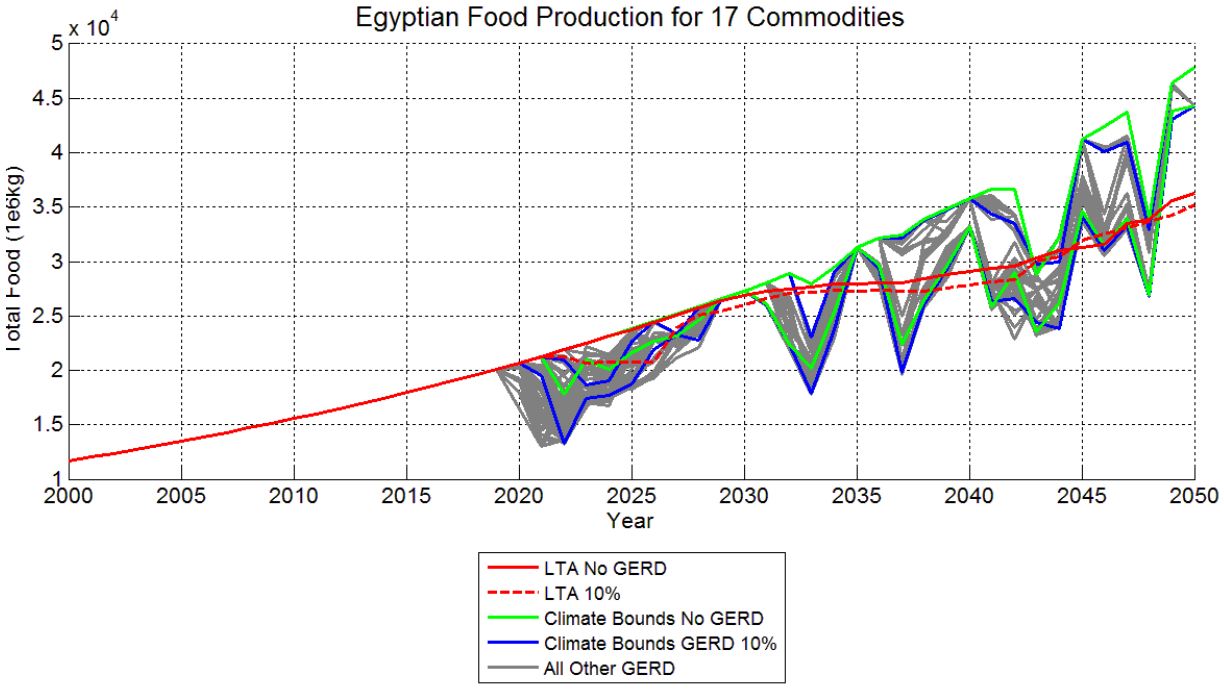

Figure 4. Total Egyptian Food Production for 17 Commodities for 80 Runs of WWAM

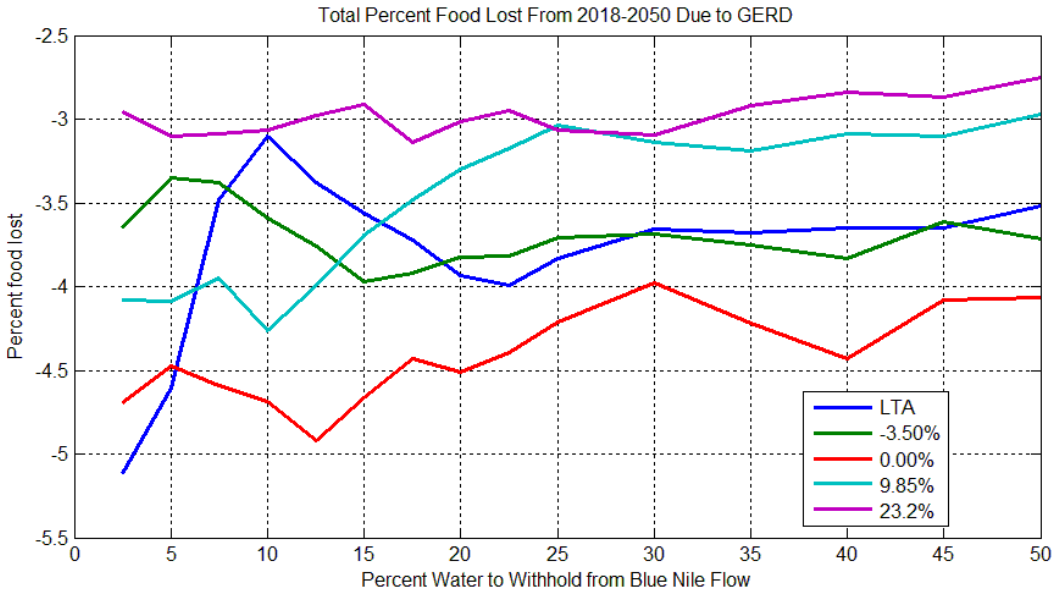

Figure 5. Total Food Lost Due to GERD for the Runoff Scenarios

1. INTRODUCTION

The Grand Ethiopian Renaissance Dam (GERD) is scheduled to be completed by 2017 to 2018. The GERD has tremendous potential for power generation in Ethiopia, yet it requires more than a year's worth of flow from the Blue Nile River, which Egypt depends on for agriculture, industry, energy, and urban/domestic uses. The World Water and Agriculture Model (WWAM) (Backus et al. 2012) has been used to focus on potential future scenarios for filling the GERD. A preliminary set of results are presented in this paper to provide a useful perspective. The WWAM was derived from a combination of the Water Simulation Model (WSM) (Cai and Rosegrant 2001) and the International Food Policy Research Institute's (IFPRI) International Model for Policy Analysis of Commodities and Trade (IMPACT) (Rosegrant et al. 2008). WWAM has a fine enough resolution to be able to accomplish food and water studies at the country/basin level. The key difference between WWAM from the original WSM and IMPACT models involves replacing optimization techniques with system dynamics decision algorithms as seen in Figure 6.

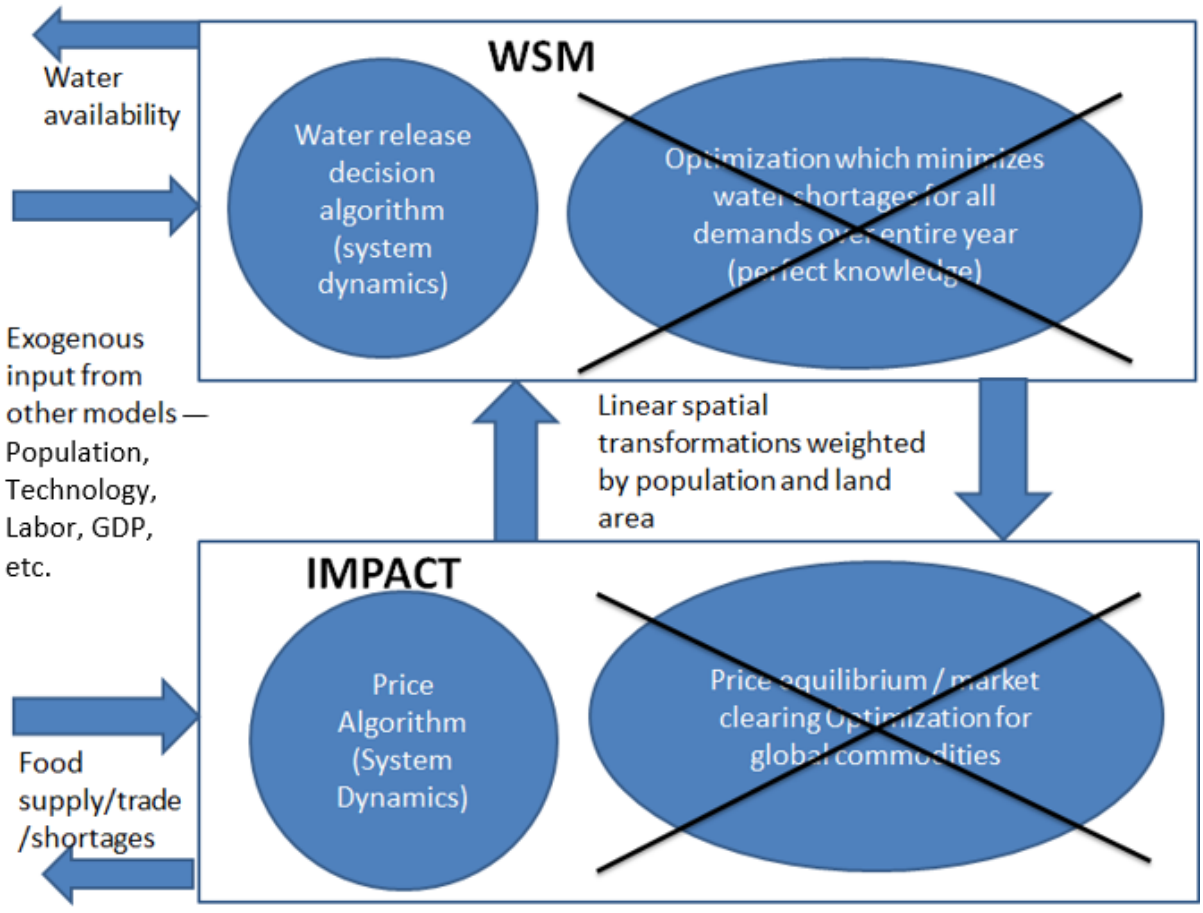

Figure 6. Changes to WSM-IMPACT to create WWAM

This approach has given WWAM an order of magnitude faster run time. In addition, the underlying theory behind the system dynamics in WWAM is better suited to handle transient shocks than the optimization techniques originally employed by WSM and IMPACT. For this study, a percentage of the stream flow of the Blue Nile River is withheld even if Egypt's water allotment of 55.5km^3 is not met. Sixteen cases were run from 0% to 50%. A second parameter dimension is added in five scenarios developed from estimates of future runoff in the Nile River Basin in the literature, long term average (LTA) data from the global runoff data center (GRDC) and from the Intergovernmental Panel for Climate Change (IPCC) Coupled Model Inter-comparison Project phase five (CMIP5) Representative Concentration Pathways 8.5 (RCP 8.5) climate scenario (Taylor et. al., 2012). This scenario represents a high emissions future. The Geophysical Fluid Dynamics Laboratory (GFDL) model was selected from CMIP5 for this study.

2. MODEL DESCRIPTION

WWAM has 282 FPUs which were formed by the intersection of 117 political regions and 126 river basins. The global map of these divisions is shown in Figure 7. The FPUs provide a sufficient level of resolution to investigate impacts caused by Ethiopia's plans to fill the GERD. The FPU's which are included in the Nile River basin and the flow of water through them, are shown in Figure 8.

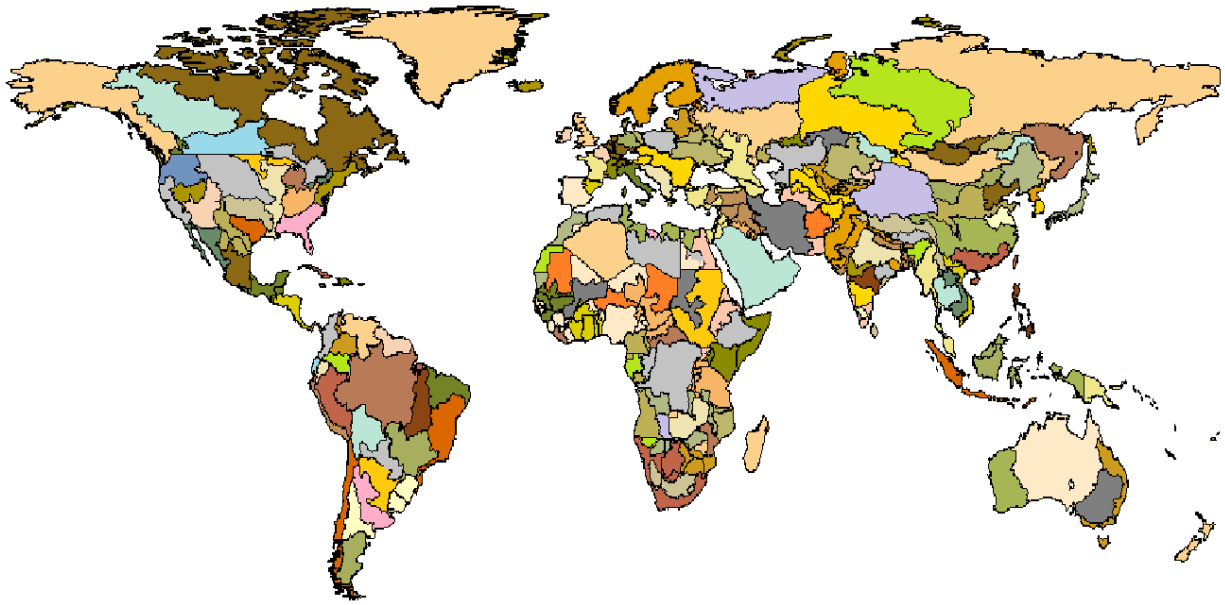

Figure 7. WWAM FPUs which are the same as for WSM

Each FPU has a water balance which lumps all water flows and storage for a large geographical area as seen in Figure 9. For the water sector, the model has a monthly time step using Euler integration. Unless noted otherwise, balance equations are the same as those proposed by Ximing Cai and Mark Rosegrant (Cai and Rosegrant, 2002).

WWAM's water demand prioritization algorithm has been constructed to allow a hierarchy of demands to be satisfied based on a limited water supply and depletive fractions for each demand type. It is described by Backus et al. (Backus et al. 2012: section 7.3) and requires the input of a matrix whose columns represent specific demands. For the present study, constant matrices for demand prioritization were used.

WWAM uses Cobb-Douglas type functions to assess crop areas, and yields to calculate supply and demand which are a function of prices of competing commodities. With this information, and a projection of water expected, a crop area is calculated for irrigated and rain fed crops. The area is reduced from the economic area desired if a water shortage is occurring. The resulting crop area and water received are then used to calculate a yield per area based on crop coefficients. These results are then calculated in a system dynamics price algorithm which

approximates market clearing, but allows supply and demand mismatches. WWAM currently has 17 food commodities: beef, pork, sheep, poultry, eggs, milk, rice, sugar, wheat, corn, other grains, soybeans, potatoes, sweet potatoes and yams, cassava and other roots and tubers, meals, and oils.

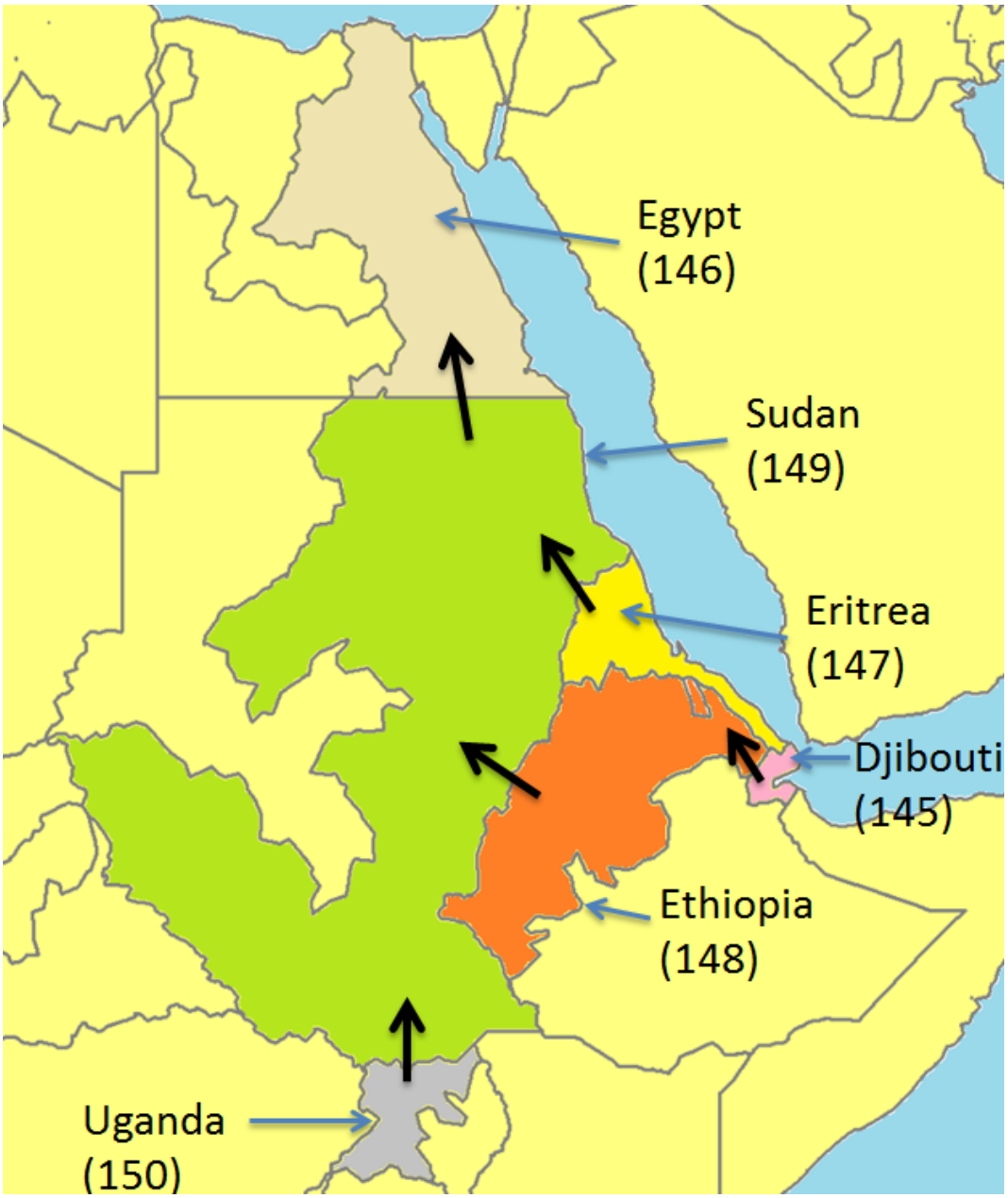

Figure 8. FPUs for the Nile River Basin

Price is determined using a linear prediction of growth in supply and demand on a one-quarter-year time step. Supply will equal demand if the resulting linear projection matches the future. This allows mismatch between supply and demand which can lead to waste of products if they are unused for their shelf-life. The world prices are translated into consumer, intermediate,

and producer prices which reflect local food policy for each FPU and are used in the supply and demand functions. Trade is prioritized for each FPU proportional to the product of Gross Domestic Product (GDP) and total food shortages. The highest product country fills its shortage first and each subsequent country meets its shortage until any surplus runs out.

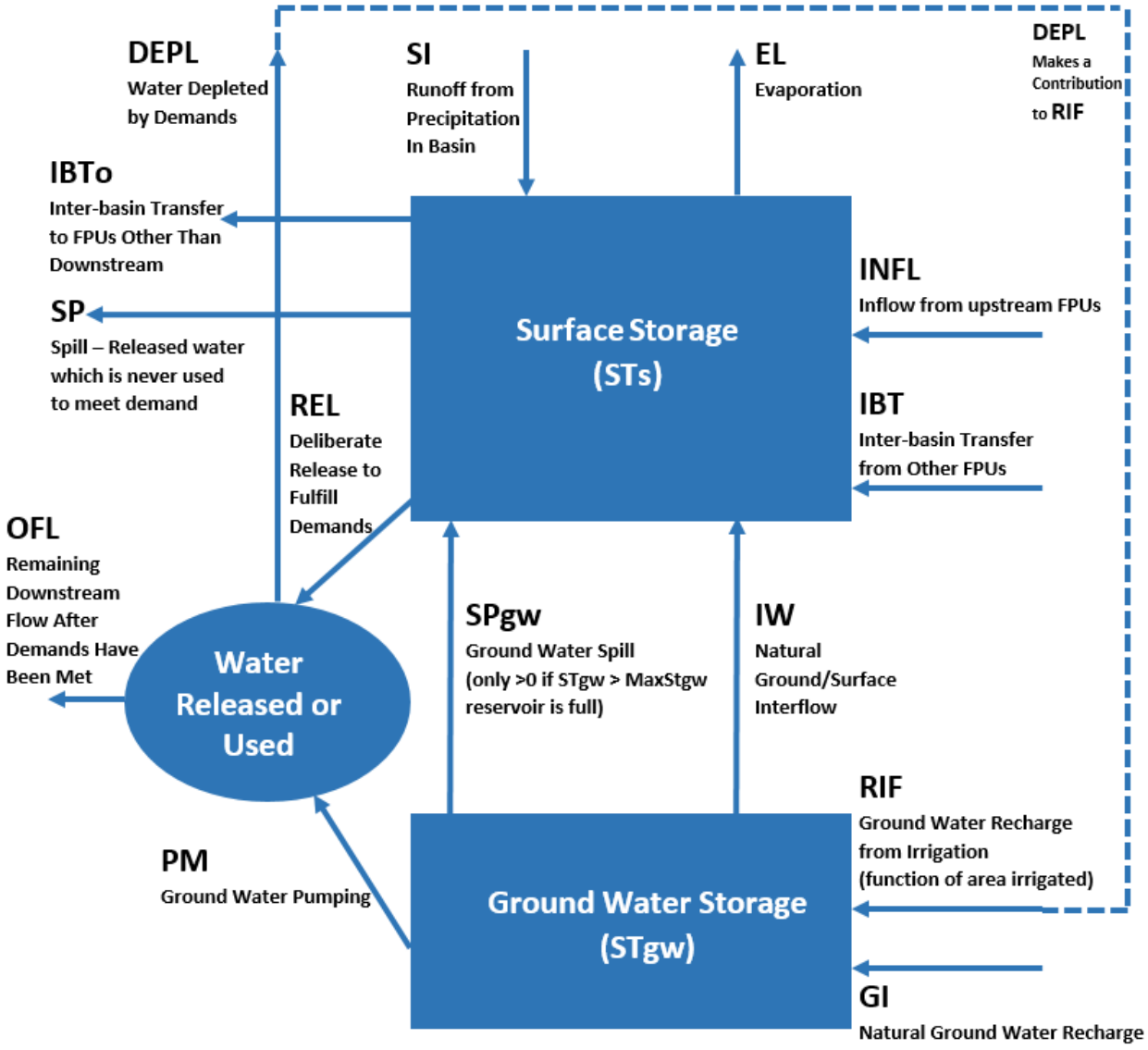

Figure 9. FPU Water Mass Balance Flow Diagram

This Page is Intentionally Left Blank

3. INPUT DATA AND CALIBRATION

WWAM needs to be calibrated further before confidence can be placed in the global results. The Egyptian results are expected to have greater accuracy, but these results are coupled to the global market which can play a significant part in the outcome of the local results. The original datasets for IMPACT and WSM were used for all FPUs outside the Nile River Basin. This includes a vast array of price, labor, supply, and demand data for water and agricultural. The accuracy of global results has not undergone calibration since the work in the early 2000s by Ximing Cai and Mark Rosegrant (Cai and Rosegrant 2001). Local updates to the Nile River Basin FPUs for Egypt, Sudan, and Ethiopia were made to ensure that inputs for these regions are more accurate. Uganda, Eritrea and Djibouti were left unaltered since their contributions are relatively minor. The following sections report the current state of the inputs to WWAM for this study.

3.1. Water

3.1.1. Supply to Demand Prioritization

The water demand algorithm orders demands by priority and then by level. The present study's values for all FPUs are shown in Table 1. In a water shortage, this mixture reflects a relatively weak (20%) commitment to downstream flows and environmental flows until 80% of a given FPU's other demand types have been met. Since other demands are relatively small in comparison to agriculture, they are satisfied first since they have the potential for affecting a larger portion of the populations involved in the short term. The 1959 Nile Waters Agreement is a committed downstream flow for Ethiopia which consumes 95% of Ethiopia's available water from the Blue Nile. Even though this commitment is included, filling the GERD and 80% of Ethiopia's demands have higher priority. Development of groundwater and other water extraction technologies are held constant for the entire scenario.

Table 1. Demand Prioritization and Level Matrix

Level	1st Priority: Downstream Commitments	2nd Priority: Municipal	3rd Priority Livestock	4th Priority Industrial	5th Priority Agriculture	6th Priority Environmental Flows[1]
Level 1	0.2	0.8	0.8	0.8	0.8	0.8
Level 2	0.8	0.2	0.2	0.2	0.2	0.2

[1] These represent cases where an environmental flow requirement exceeds downstream commitments.

3.1.2. Demand

WAMM follows WSM's original format by dividing water use into agriculture, livestock, municipal and industrial sectors. The agriculture demand is calculated as a function of LTA climate data, effective efficiency of the basin, the relative price of water, and crop areas calculated by IMPACT. These crop areas are functions of price competition between alternative crops, crop area availability and growth, and of previous areas planted. The demand is calculated as the maximum beneficial water to each crop type. The crop area and yield are reduced if the demand cannot be met. This adjustment process is described by Cai and Rosegrant (Cai and Rosegrant, 2002).

$$DA_{y,m,u} = 0.01\sum_{c}\left[AI_{y,u,m,c} \otimes \left(ETP_{u,m,c} - PEF_{u,m,c}\right) \otimes \frac{1}{EE_{u,c} RWP_{u}^{\epsilon_u}}\right] \quad (1)$$

In this equation, *DA* is the total agricultural demand in cubic kilometers for all crops[2]; *AI* is the irrigated area calculated by IMPACT in million hectares (10^{10} meters squared); *ETP* is the long term average potential evapotranspiration of the current crop and month in millimeters; *PEF* is the long term average effective precipitation in millimeters; *EE* is the effective efficiency for the current crop and FPU (Cai, 2002); *RWP* is the relative price of water, and ϵ is the price elasticity for the *RWP.* The $\otimes$ operator indicates an element-wise multiplication of the matrices for shared indices which are not being summed. For dimensional mismatches between the arrays involved, the elements of the array with lower dimensionality are repeated for each unmatched index of the higher order array. The *c* index is for crops which include the crop type commodities listed earlier, the *u* index stands for the 282 FPUs, the *m* index represents the month, and the *y* index stands for the range of years simulated. For the present study, the relative price of water (*RWP*) has been assigned a value of one for all years and FPUs.

Livestock is also a function of IMPACT's output. IMPACT divides livestock between animals slaughtered for production of meat and animals which are being kept alive for animal products or future slaughter. The living animals produce a demand proportional to their numbers.

$$DL_{y,m,u} = 10^{-6}\left(\sum_{a} AL_{y,u,a} WU_{u,a}\right) \otimes dl_{u,m} \quad (2)$$

where *DL* is the actual demand for livestock by year, month and FPU*; AL* is the total mass of livestock from IMPACT for a given year, FPU, and livestock type; *WU* is the water use per livestock given livestock type and FPU; and *dl* is a vector that distributes the yearly demand to each month. It represents the fraction of use for each month across all livestock types.

[2] The factor 0.01 is necessary to produce the correct units. Unfortunately, WWAM did not inherit a consistent set of units from WSM-IMPACT. In addition, there is not even consistency between IMPACT and WSM. For example, IMPACT has units of area of 1,000 hectares, whereas WSM has units of 1,000,000 hectares.

Municipal and Industrial water uses are more simple since they are not tied to IMPACT outputs. Both are represented by Cobb-Douglass type functions for demand. The municipal demand is represented as a function of population and GDP. Both of these are exogenous outputs to WWAM presented in section 3.2.[3]

$$DM_{y,u,m} = DM0_{u,m}\left(\frac{POP_{u,y,m}}{POP0_u}\right)^{\alpha_u}\left(\frac{GDP_{u,y,m}}{GDP0_u}\right)^{\beta_u} \quad (3)$$

where *DM* is the municipal demand, *DM0* is the initial municipal demand, *POP* is the population, and *GDP* the gross domestic product. α and β are demand elasticity constants which have been set to 1 for population and 0.5 for GDP. These values were chosen to make the growth into the future reasonable. For future studies, it would be desirable to obtain more detailed historical data which would allow their calibration. Industrial water demand is unaltered from the original model proposed by Cai for WSM (Cai, 2002).

For Egypt, initial demand in 2000 was set according to the estimated percentage breakdown given by Strzepek and Yates with 89% going to agriculture, 7% to domestic, and 4% to industry. Livestock was given a portion of the industry's 4% water allotment (Strzepek and Yates 2000). These percentages were multiplied by the Food and Agriculture Organization (FAO) of the United Nations (UN) estimate for total water consumption in Egypt equal to 58.3km^3 (FAO 2004).

3.1.3. Depletion Fractions

Based on data from the FAO (FAO 2004) presented in Yang et. al. (Yang et. al. 2007), the total water used in Egypt in 2000 was estimated to be 68.65km^3 whereas the total renewable water resources were estimated to be 58.3km^3. This means that approximately 17.75% of the renewable water resources were recycled. The WWAM model was therefore assigned depletive factors of 82.25% for Egypt and this same number was also used for all other FPUs. The FAO data set could be used in the future to make an estimate for each FPU in the model for the depletive factor.

3.1.4. Fill Rate of GERD and Rule Curves

In addition to demand prioritization and depletive factors, a rule curve was introduced to address two situations. The first situation involves spilling additional water beyond demands in order to reach a target level. A sinusoidal curve was used on all of the countries with a rule curve which reaches its annual low point on August 1st with a reservoir level of no more than 87.5% of capacity which is 140 km^3 for all water in Egypt's Nile River Basin. This corresponds to the policy communicated by Hossain and El-Shafie (Hossain and El-Shafie 2014: 1202) and

[3] This means that municipal demand is a calculated exogenous variable with no feedback. Livestock and Agricultural demands have feedback between the food and water models.

constrains all reservoirs in Ethiopia, Sudan, and Egypt to release excess water to avoid uncontrolled spill during the Blue Nile River annual flood.[4]

The second situation which uses a rule curve happens when the current time step's storage will fall short of the rule curve storage target because demand is too great. When this is the case, the user can specify that a percentage of the available stream flow into the current FPU be withheld. This condition was used to simulate a demand to fill the GERD above all other demands. The maximum storage of Ethiopia was increased by 63km^3 at the end of 2018. The model automatically scales to this new storage capacity and a specified percentage of total inflow minus evaporation for the Ethiopian Blue Nile Basin is withheld if the water levels are below the rule curve.

3.1.5. Climate Data

The climate runoff data was derived from IPCC CMIP5 GFDL RCP 8.5. The yearly, long-term average of the climate data from 2006 to 2050 indicates 2.5 times as much water compared to the historical (1961-1997) long term average from the Global Runoff Data Centre (GRDC)[5]. In addition to this, the distribution of water throughout the year for the Blue Nile River has a noticeable difference in shape as illustrated in Figure 10 where the long term average from 2006-2050 compared to long term average from 1961-1997 is based on historical data at Roseires.

[4] Remember that WWAM is representing all water and is not a model of individual reservoirs. Lake Nasser is supposed to reach a level of 122km^3 on July 31st according to Hossain and El-Shafie.

[5] The authors did not access this information directly, but the website for IWMI was found at http://wcatlas.iwmi.org/default.asp and the website for GRDC is http://www.bafg.de/GRDC/EN/Home/homepage_node.html (both accessed 9/12/2014)

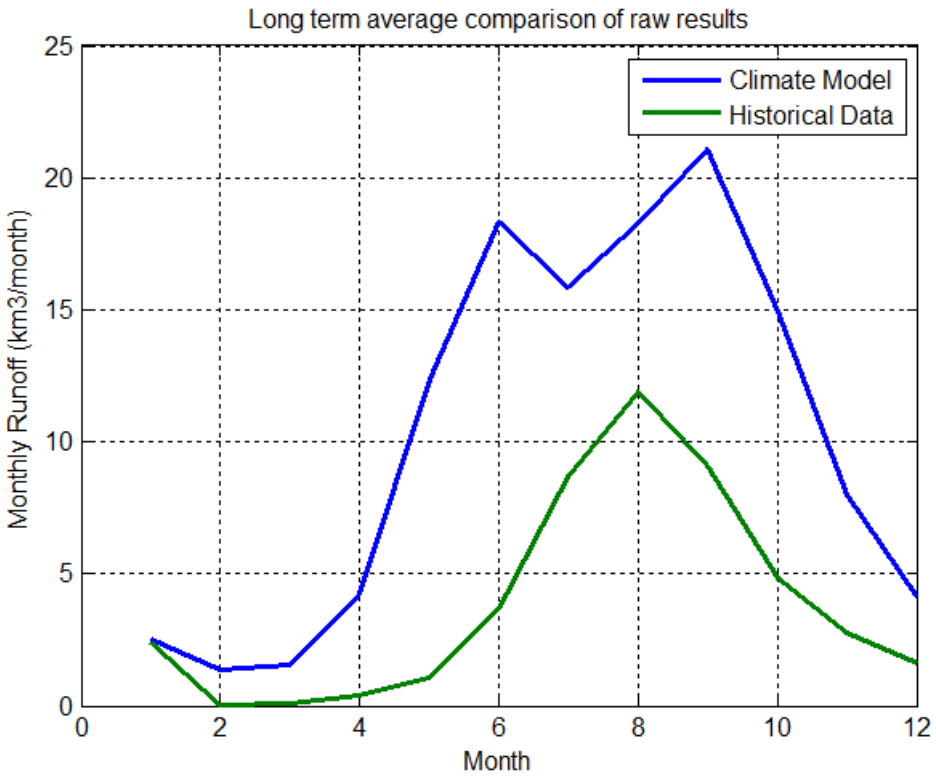

Figure 10. Blue Nile River Climate Model

It was assumed that the climate model data contains the best available statistical averages concerning future trends in global runoff. Currently, this effort has not yet obtained direct access to enough historical runoff data to be able to perform downscaling as presented by Elshamy et. al. or Hwang and Graham (Elshamy et. al. 2009, Hwang and Graham 2014).

Quantifying changes in runoff due to climate change is a highly uncertain process because of complex interactions between clouds, wind, evapotranspiration and precipitation which are areas of active research. The Blue Nile River is the largest contributor to inflow at the Aswan High Dam and has been estimated to have a sensitivity scale of 2 (Aich et. al. 2014) to 3 (Elshamy et. al. 2009, Conway and Hulme 1993, Sayed 2004) for changes in precipitation. This means that a 10% increase in precipitation can result in an increase of 20-30% in runoff. Sensitivity of potential evapotranspiration is smaller with a factor of 1.4 estimated by Elshamy et. al. (Elshamy et. al. 2009: 558).

Temperature rises have much better certainty with respect to climate predictions from current General Circulation Model (GCM) results. According to Elshamy et. al., changes in precipitation for the Blue Nile River are +15% to -14% for the IPCC CMIP3 Assessment Report 4 (AR4) data set using 17 GCMs with an average change falling very close to 0% change in precipitation. The models used indicate a temperature rise which causes evapotranspiration to increase, which Elshamy et. al. argue will subsequently lead to decreases in runoff in the Blue Nile River of 3.5% for the ensemble mean versus historical data from 1961-1990. Beyene et. al. reversed the sign

of this assessment with a different analysis of IPCC AR4 data for precipitation and temperature (Beyene et. al., 2010). The simulated stream-flow increased by 10% for a comparison of 1950 to 1999 historical averages to 2010 to 2039 averages for 11 GCMs used.

Using the more recent CMIP5 dataset, Aich et. al. forecast that the Blue Nile River will experience a 56-57% increase in peak discharge rates and 18-21% increase in lower level discharge rates for the 2020 to 2049 time interval. Yet, in a more globalized assessment, Alkama et. al. observe that a combination of CMIP5 experiments and stream flow observations are, "found to simulate the climatological stream flow reasonably well, except over South America and Africa." (Alkama et. al., 2013).

It is therefore anticipated that a simplified bias elimination procedure will not lead to unreasonable climate scenarios because of the inherent uncertainty of future stream flows in the Nile River Basin, lack of information to do more sophisticated bias elimination, and WWAM's coarse hydrological resolution.

For each month, the historical long term average runoff was multiplied by the climate model runoff. For each year, this result was then normalized to a total sum of one. This first resulting time series was then multiplied by the total long term average runoff for the interval 1961 to 1997 (Sutcliffe and Parks, 1999) of 46.4km^3/yr. at Roseires. This second resulting time series was then multiplied by the ratio of the climate data's total runoff to the long term average runoff. This final resulting time series has a long term average equal to the historical long term average, but it contains yearly variations which are proportional to the climate model's variations. Equations 4 and 5 summarize these operations

$$FR_{umy} = F_{Yuy} \frac{CD_{umy} HR_{um} \sum_{n=1}^{12} HR_{un}}{\sum_{n=1}^{12} CD_{uny} HR_{un}} \tag{4}$$

$$F_{Yuy} = \frac{(2050 - 2005) \sum_{n=1}^{12} CD_{uny}}{\sum_{i=2006}^{2050} \sum_{n=1}^{12} CD_{uni}} \tag{5}$$

where CD is the climate data, HR is the historical long term average runoff from GRDC, $F_Y$is the yearly scaling factor relative to the climate data long term average, u is the set of 282 FPUs, y is the set of years 2006-2050, and m represents each month of the year. $FR_{umy}$is the desired

future runoff scenario. This resulting dataset still has the original climate data's proportional trends on a yearly scale, but it requires an offset which indicates a climate change. In light of the high uncertainty of runoff forecasts for the Nile River Basin, it is reasonable to form five scenarios which explore the bounds of reported behavior in the literature surveyed earlier by developing the following cases:

1. Long term average runoff
2. Climate data with 3.50% less runoff than the long term average over 2006-2050 (Elshamy et. al., 2009)
3. Climate data with 0.00% change from the long term average over 2006-2050 (Climate variation with 0 net change to long term average)
4. Climate data with 9.85% more runoff than the long term average over 2006-2050 (Average of Elshamy and Aich et. al.)
5. Climate data with 23.2% more runoff than the long term average over 2006-2050 (Aich et. al.)

These scenarios do not represent extreme bounds of possibility, but they provide enough variability to consider whether conclusions about GERD filling scenarios are robust with respect to climate uncertainty. Figure 11 shows the resulting runoff scenarios generated.

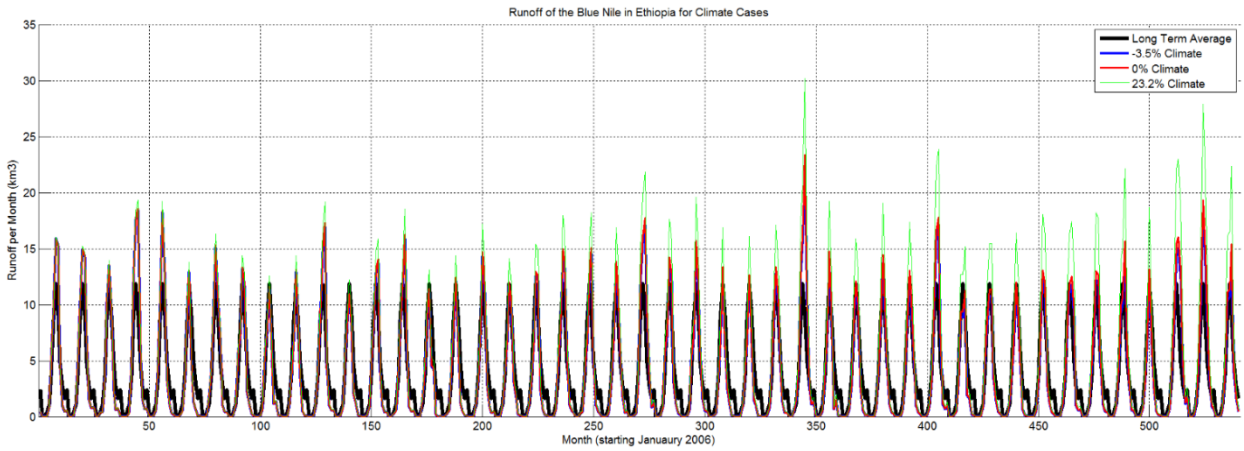

Figure 11. Runoff Scenarios Generated

Evaporation was evaluated monthly based on long term potential evapotranspiration of each FPU multiplied by the surface area for the current reservoir storage in each country. WSM's long term potential evapotranspiration data comes from the International Water Management Institute (IWMI) as seen in Figure 12.

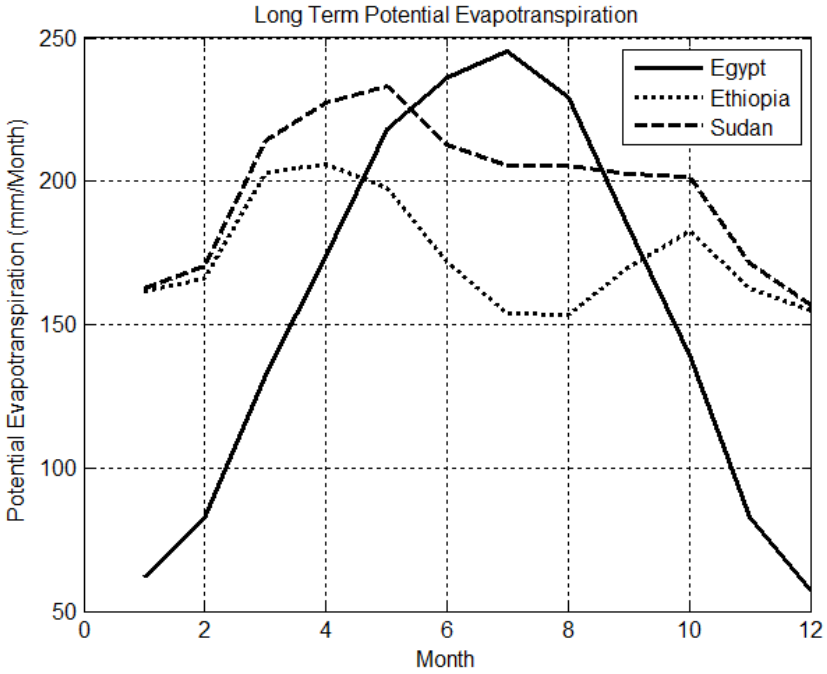

Figure 12. Long Term Average Potential Evapotranspiration from IWMI

3.1.6. Hydrology and Bathymetry

For hydrological balances, Lake Nasser levels were obtained using the Hydroweb database (Crétaux, et al. 2011). Bathymetry for Lake Nasser's water basin was found in Hossain and El-Shafie equations 8 and 9 (Hossain and El-Shafie, 2014).

$$E = 79.97 + 0.0369V + 18.87\ln(V) \quad (6)$$

$$A = -3164.28 + 25.49V + 1092.92\ln(V) \quad (7)$$

where *E* is elevation in meters, *A* is the lake surface area, and *V* is the volume of water. These bathymetry levels were compared to the bathymetry found in Muala et al. (Muala et al., 2014) and were found to be comparable. In order to simulate very low levels in the reservoir, a linear extrapolation to zero was used whenever water levels in Egypt drops below 28.86km^3 as shown in equation 8.

$$A = \begin{cases} 1246\left(\frac{V}{28.86}\right) & V \leq 28.86km^3 \\ -3164.28 + 25.49V + 1092.92\ln(V) & V > 28.86km^3 \end{cases} \quad (8)$$

The bathymetry for GERD was taken directly from King's equations 5 and 6 (King 2013: 17) as seen in equation 9. The volume in this case is in million meters cubed while the surface area is still in kilometers squared.

$$A = \begin{cases} -3.0 \cdot 10^7 V^2 + 0.0466V & V < 15{,}000km^3 \\ -3.0 \cdot 10^7 V^2 + 0.046V - 28.6 & V > 15{,}000km^3 \end{cases} \quad (9)$$

The bathymetry for the Sudd Wetlands and Sudan's Nile River Basin is not as well quantified and is continually changing. Based on Mohamed and Savenije and Sutcliffe and Parks, the bathymetry of the Sudd Wetlands has nearly zero incline and has approximately doubled in size in the last 100 years (Sutcliffe and Parks, 1999, Mohamed and Savenije, 2014). The linear area to volume slope was therefore allowed to be a calibrating factor in the model which was adjusted to make historical levels in Lake Nasser approximately equal to the average response in WWAM. Due to lack of information on bathymetry, a bilinear function was used as shown in equation 10.

$$A = \begin{cases} 1.06e7\left(\frac{V}{92}\right) & V \leq 92km^3 \\ 1.06e7 + 5e4(V - 92) & V > 92km^3 \end{cases} \quad (10)$$

3.2. Population and Gross Domestic Product

The population and GDP data comes from an unpublished composite of future UN population growth rates and historical World Bank data (World Bank, 2014) from 1960 to 2100. For future years, the series developed are according to the UN IPCC 2007 4th assessment report with further processing to make GDP consistent with population by the Center for International Earth Science Information Network at Columbia University (CIESIN, 2002). The combined historical data and projected future were scaled to make a continuous time history useful to system dynamics models by George Backus at Sandia National Laboratories. The resulting population and GDP time series for the countries of interest from 2000 to 2060 are provided below in Figure 13. These signals affect water and agricultural demands in WWAM.

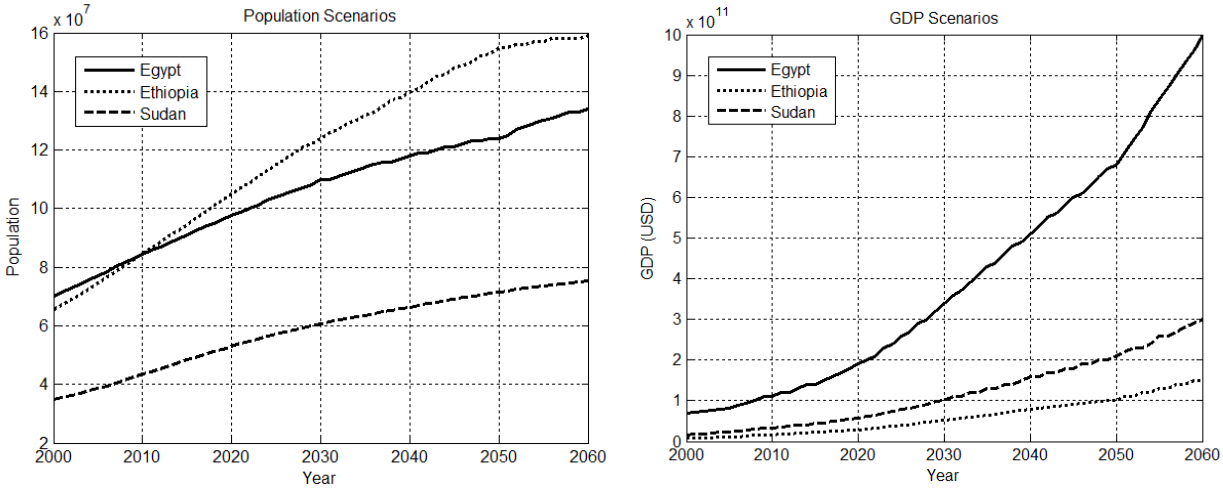

Figure 13. Population and GDP Scenarios

3.3. Hydroelectric Power

Hydroelectric power was simulated for Aswan High Dam and the GERD power station. Modeling for the Aswan High Dam comes from a regression of the Awan High Dam power generation produced by Abdelsalam et. al. using data from 1988 to 2000 (Abdelsalam et. al., 2008).

$$P = -689.41 + 0.167Q + 9.62z \qquad (11)$$

P is the average power output over a month of time in megawatts, *Q* is the discharge through the turbines in millions of cubic meters per month, and *z* is the head in meters. The head is one-to-one with the elevation in equation 6 with an offset equal to the turbine height which is listed by Donia as 108 meters (Donia, 2013).

$$z = E - 108 \qquad (12)$$

For the GERD, a simple energy potential exchange model was used since actual performance data does not exist (King, 2013).

$$P = \eta_T \rho Q z \qquad (13)$$

Following King's lead, the turbine efficiency, η_T, was assigned a value of 0.95 and the specific gravity of water, ρ, was set to a constant equal to 9,807 Newtons per cubic meter. The release, *Q*, is in million meters cubed per second and the head, *z*, is in meters to produce power output in megawatts. The head was calculated according to the fit used by King of head versus storage (King, 2013).

$$z = 7.282V^{0.268} \quad (14)$$

For both the GERD and Aswan High Dam, the power output was multiplied for the duration of the month to produce a final assessment of energy generation in gigawatt-hours.

3.4. Technology and Agricultural Growth

WWAM is identical to IMPACT in these areas and assumes six periods of constant growth (or decline) as seen in Figure 14. These simple assumptions can easily be changed to a time series which is based on another model exogenous to WWAM.

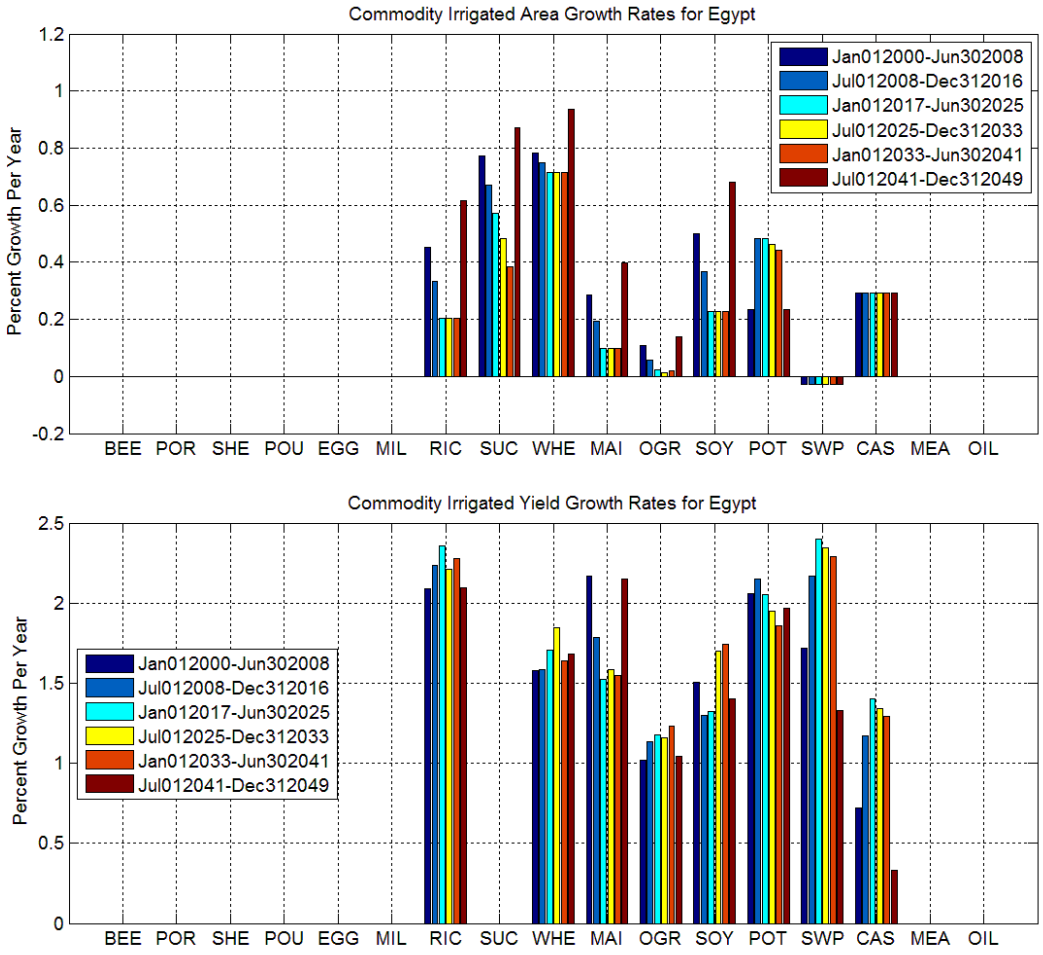

Figure 14. Yield and Area Growth to WWAM's 17 Commodities

This Page is Intentionally Left Blank

4. RESULTS

The results for this study serve to illustrate WWAM's capabilities but have not been investigated for accuracy on a global level. The results in Egypt have been verified to be reasonable, but more calibration is needed to gain further confidence.

4.1. Water Supply and Demand

The Egyptian imbalance between supply and demand is depicted in Figure 15 – Figure 18. Supply falls short of demand for all of the sectors and all the scenarios regardless of the presence of the GERD. Water stress is most severe for agriculture. The GERD begins drawing resources on Jan 1, 2019.[6] There is a one to two year delay after 2019 before Egypt starts to experience differences due to the GERD. The GERD scenarios lead to losses in agricultural supply for three to six years before the baseline scenario begins to fall below demand.

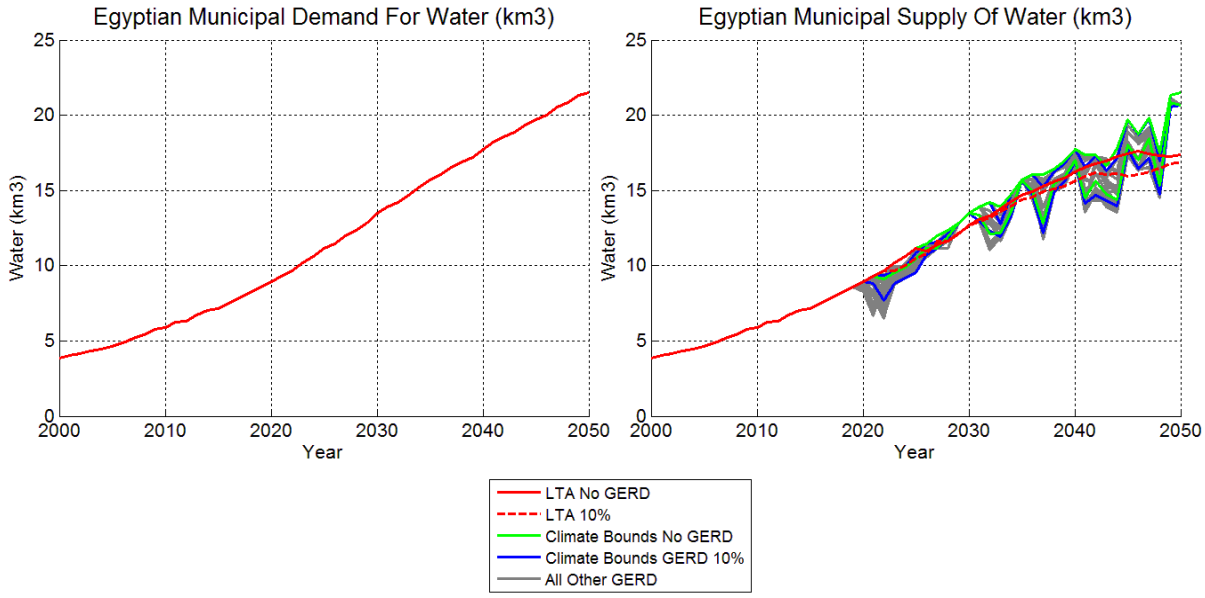

Figure 15. Egyptian Municipal Water Demand (left) and Supply (right)

[6] Each point on the graphs represents the end of the year.

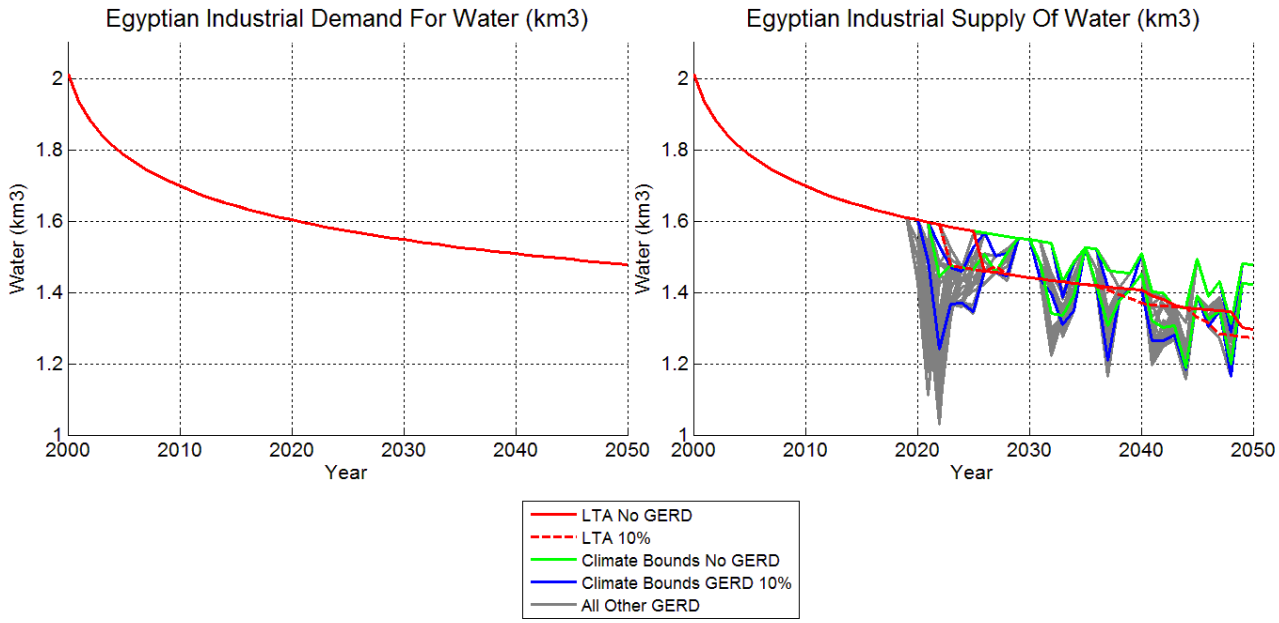

Figure 16. Egyptian Industrial Water Demand (left) and Supply (right)

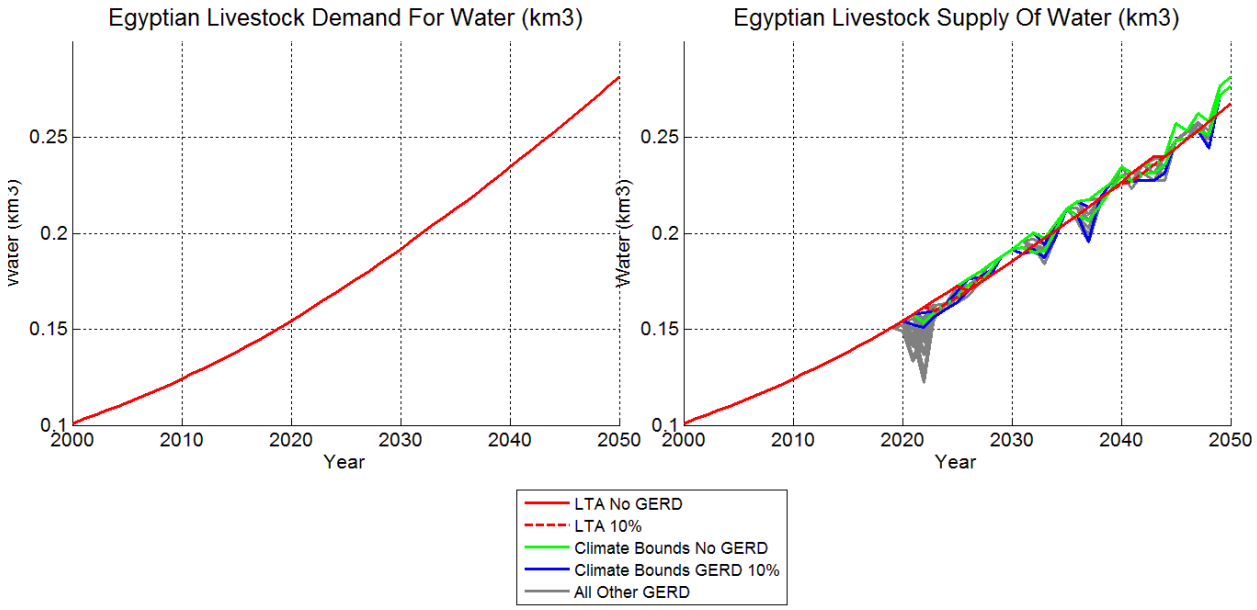

Figure 17. Egyptian Livestock Water Demand (left) and Supply (right)

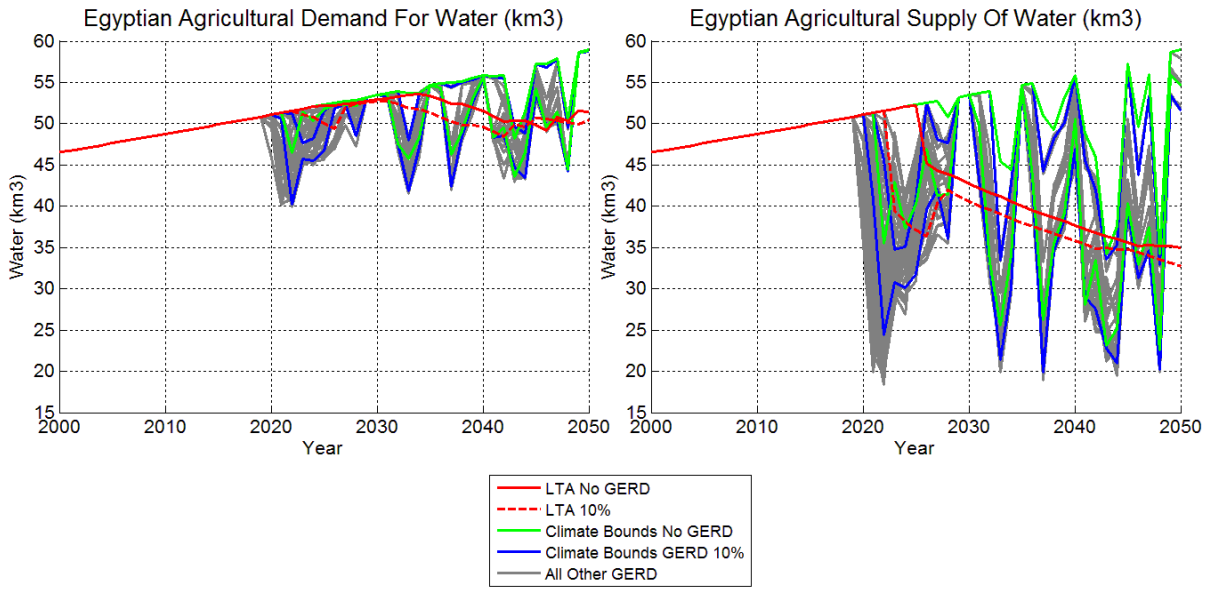

Figure 18. Egyptian Agricultural Water Demand (left) and Supply (right)

4.2. Water Balance

The total inflow to Egypt is depicted in Figure 19. The Sudanese demand starting at approximately 18km^3 is already taken away from this inflow. In addition to this, evaporation and other water balance terms have to be taken away before the actual outflow from Aswan Dam can be approximated which is not very straightforward for the lumped FPU approach WWAM uses. Figure 20 gives the yearly storage balance of Egypt. Two important indicators for the GERD filling strategy come from the monthly storage data calculated for Egypt and Ethiopia. The first is the length of time to fill the GERD reservoir for Ethiopia depicted in Figure 21. The second is the point at which Egypt reaches Lake Nasser's dead storage of 31km^3 which represents minimal power generation and no reserves to meet growing demands as seen in Figure 22.

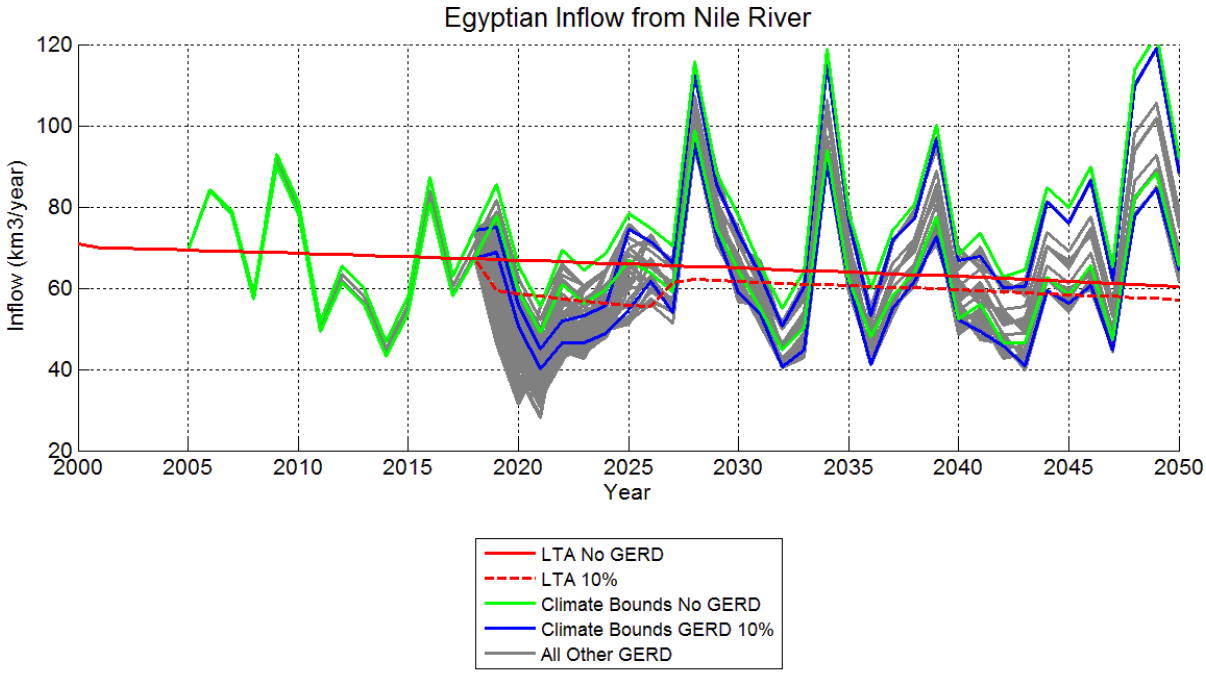

Figure 19. Egyptian Inflow from Nile River

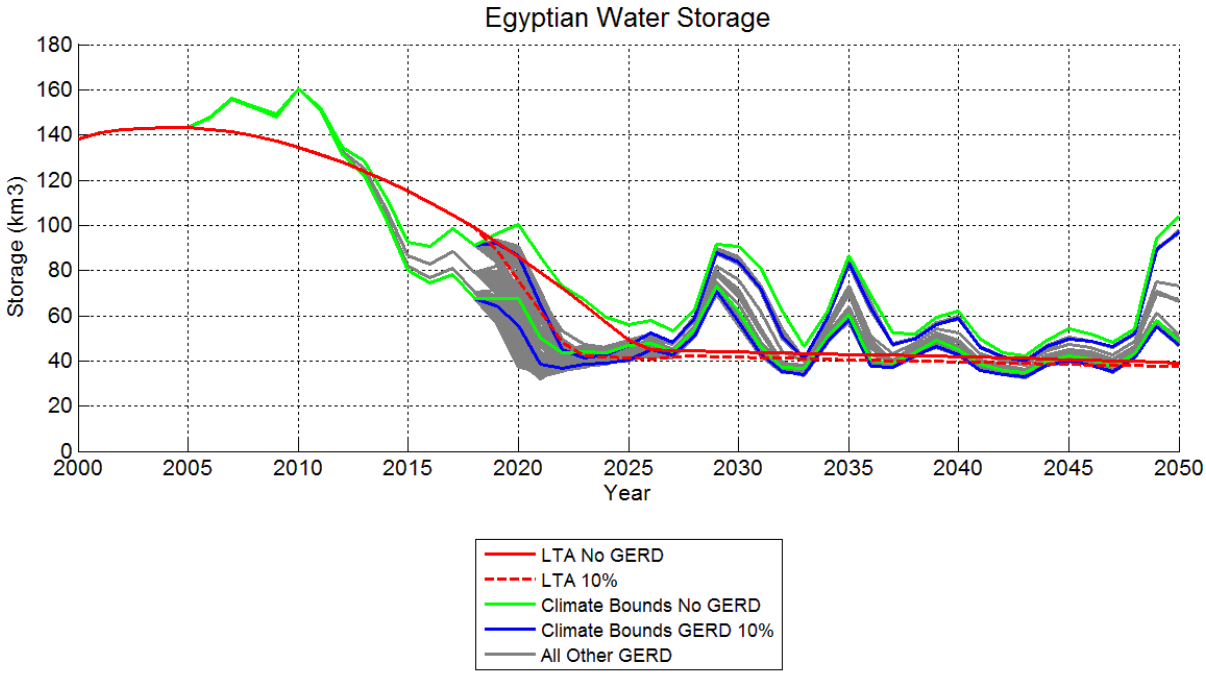

Figure 20. Egyptian Storage

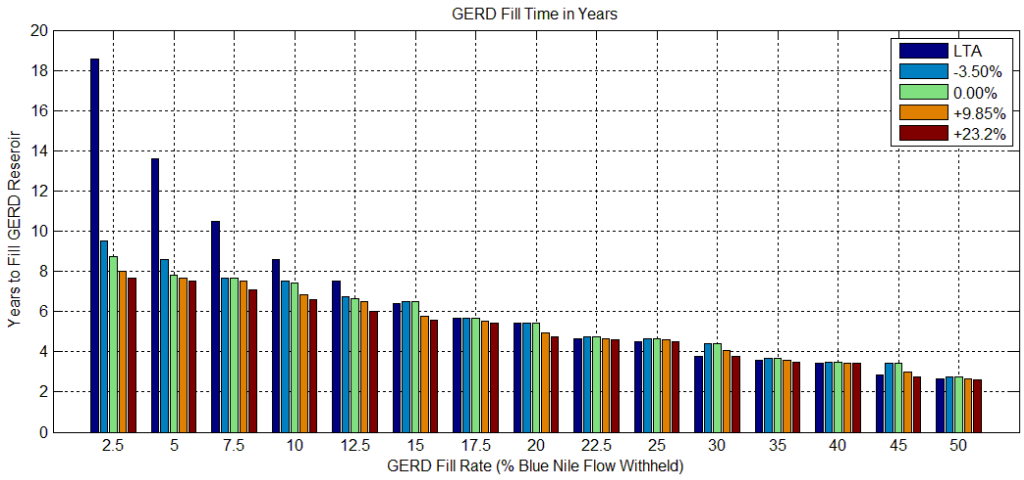

Figure 21. GERD Fill Time

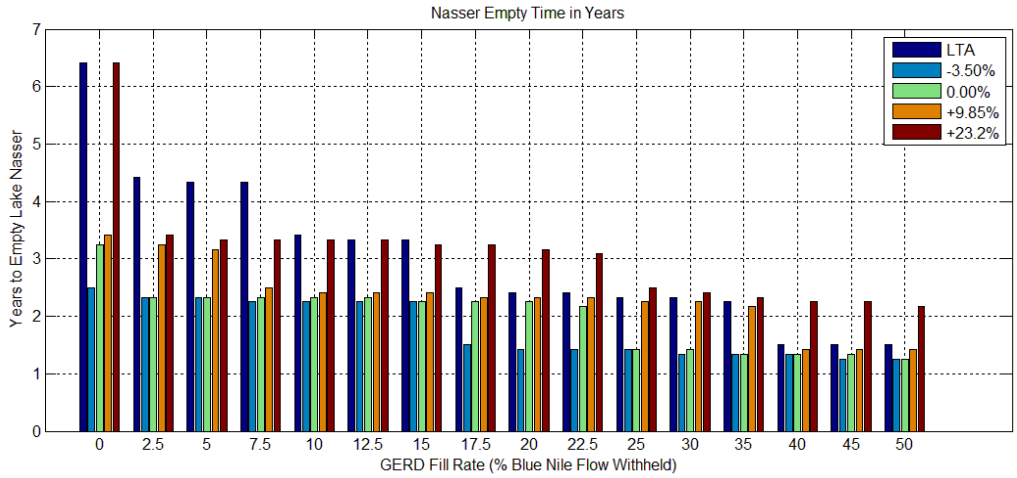

Figure 22. Lake Nasser Time to Dead Storage

Climate plays a considerable role in both of these metrics. For the slower fill rates, the time to fill the GERD stops increasing because of the sudden wet period in 2027 to 2030. For the emptying of Lake Nasser, the sudden decrease in inflow from 2019 to 2021 causes Lake Nasser to empty abruptly which overwhelms the effects of losses due to the GERD.

4.3. Evaporation

Evaporation is an affect which is tied to the bathymetry and climate of the FPUs. Figure 23 gives the total evaporation from the entire Nile River Basin in WWAM. When compared to the baseline scenario, the model indicates that the overall evaporation always increases due to the GERD. This is counter to the argument that the GERD will decrease evaporation since its

evaporation rates are lower than those for Lake Nasser. The only way that evaporation can be decreased for the overall system is to enforce very low storage in Lake Nasser and high storage in the GERD. The system is not constrained in this way and every scenario in this study with the GERD increases the overall evaporation potential by 3.2km^3. Figure 24 provides a look at these predicted increases in evaporation. Despite the predictions from WWAM, there are a number of issues which may actually reverse this conclusion. For example, the GERD could save considerable water through better regulation in flood events. As reservoirs overflow, the bathymetry in Sudan and Egypt probably is not very accurate and events such as spilling excess water into the desert could be eliminated. The WWAM results are also based on long term potential evapotranspiration which is not changing with the climate the same way that the runoff is changing.

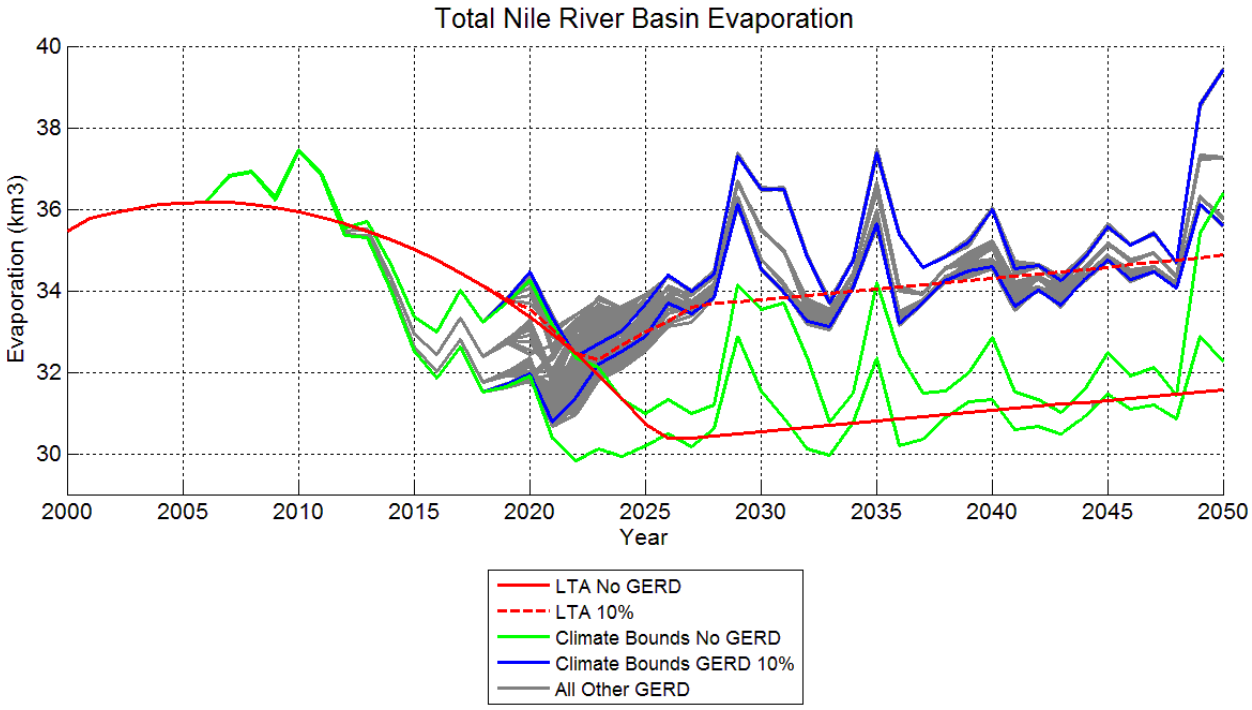

Figure 23. Ethiopian and Egyptian Losses by Evaporation

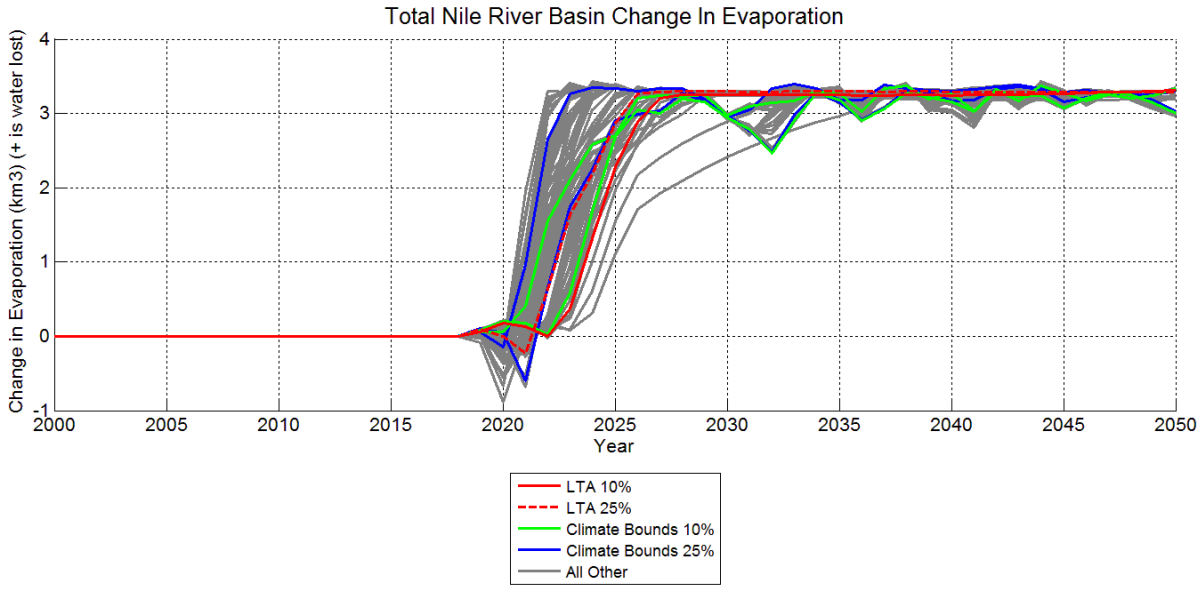

Figure 24. Increase in Evaporation Due to GERD

4.4. Hydropower

The estimated hydropower clearly portrays that the GERD produces approximately three times as much power as the Aswan High Dam. From a cross-border perspective, implementing the GERD is a huge improvement as seen in Figure 25 and Figure 26. From Egypt's perspective, the GERD is cutting their power output by a significant fraction.

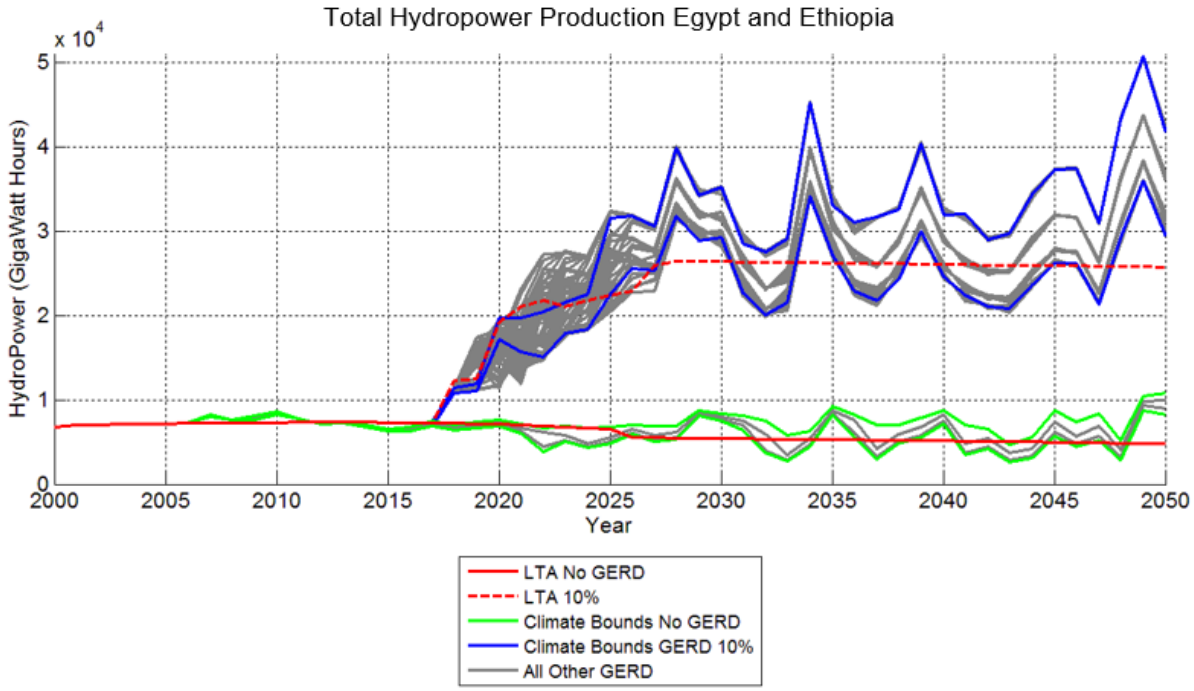

Figure 25. Hydropower Production for Egypt, Ethiopia, and Total for Both countries

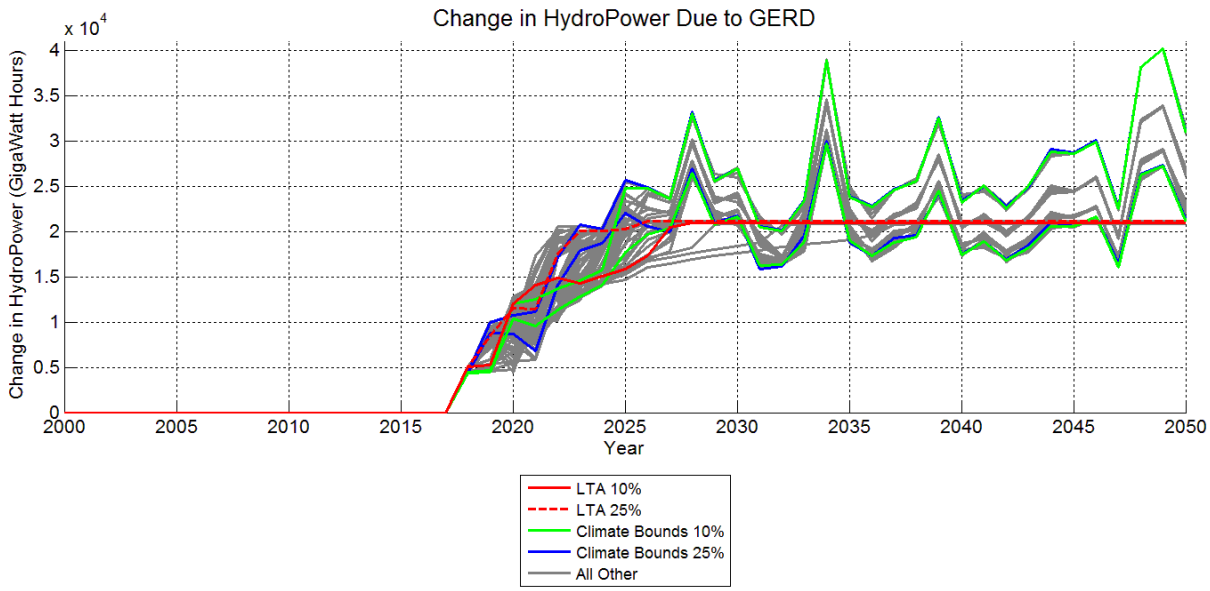

Figure 26. Increase in Power Produced Between Aswan High Dam and the GERD

4.5. Food

The IMPACT food output is still being tested. The units being used are 1e6kg of food. Modeling needs to be created which translates the caloric/nutritive value of each of the commodities to humans. Figure 27 illustrates the changes in food production for Egypt because of the GERD scenarios. Further verification and validation is needed for this output. Even though the validity of these results requires further investigation, it shows that WWAM has the capability to assess food markets for 17 different livestock and crop commodities which account for the majority of total food production in the world. If the total food is added together from 2018 to 2050, the overall effect on food production in Egypt can be quantified as seen in Figure 28.

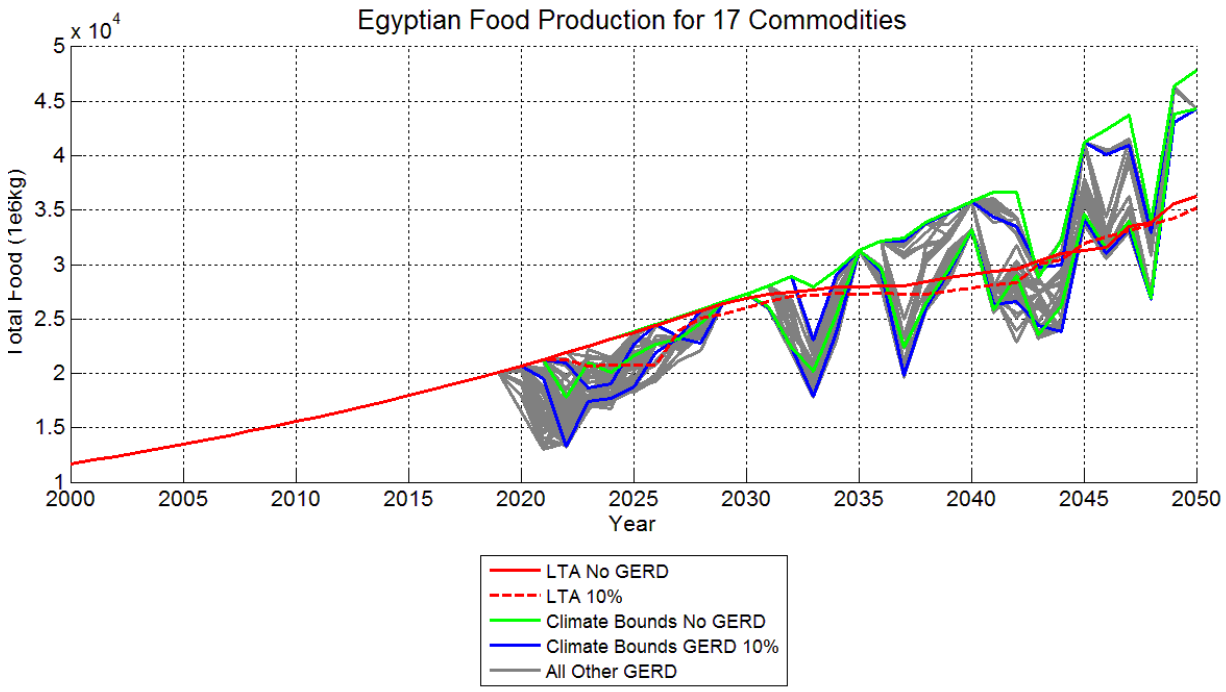

Figure 27. GERD Effects on Food Production in Egypt

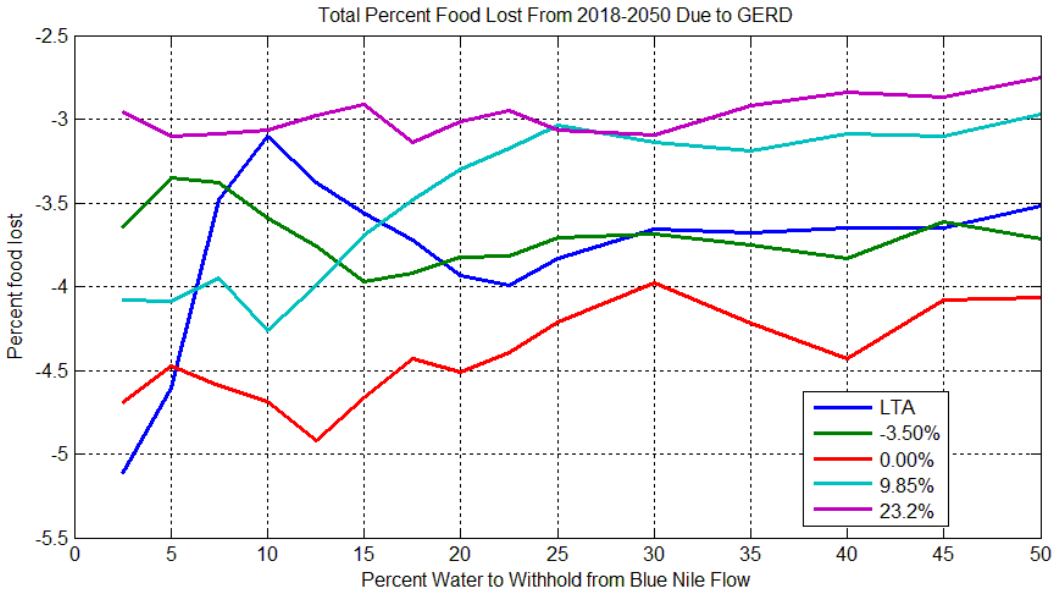

Figure 28. Percent Food Lost in Egypt Due to GERD

4.6. Discussion

As expected, GERD has a negative effect on Egypt's hydropower, agricultural, and water consumption sectors. Regardless, this negative effect is not as strong as climate uncertainty and Egypt's increases in demands due to population and economic growth. The modeling currently

completed rigidly drives forward with no feed-back for technology, population or economic dynamics. It must therefore be understood that the water conclusions reflect a policy of Egypt doing nothing beyond business as usual to amend its water stress.

The single climate data set for runoff (IPCC CMIP5 GFDL RCP 8.5) used to develop five scenarios shows how policy optimization is not straightforward because of the uncertainty of wet and dry periods inherent in climate prediction. The constant withholding of a fraction of the water is insensitive to this problem and the results suggest an approach which only withholds water when flows are exceeding the historical average stream flow as simulated by King (King, 2013: 15) would lessen negative effects of the GERD in Egypt. On the other hand, such policies could leave Ethiopia with a partially filled reservoir for decades if there is a considerable dry spell as will occur if the current draught in Ethiopia persists.

Many unknowns such as spilling flood water into shallow desert flat-lands in Egypt or Sudan could reverse the conclusions of this study concerning whether the GERD has a positive or negative impact on basin-wide evaporation. The hydropower generation produced by the GERD is a positive contribution to the entire region which will enable modernization of Ethiopia and other countries as well. In addition, there are many other positive contributions such as decreasing silt flows downstream and flood regulation which this study does not address. Negative environmental effects are also not addressed by this study.

This modeling has been the first the authors are aware of that ties losses of water due to the GERD to losses in agricultural output in Egypt. WWAM has been demonstrated to be capable of producing feasible losses in agriculture. It can now be used to combine climate uncertainty, water, food, and hydropower considerations into a single framework for evaluating a broad range of scenarios concerning the GERD and other water, food, and hydropower issues throughout the world.

5. NEXT STEPS

This work has produced the first major study using the WWAM model. There are many enhancements which are desirable.

5.1. Steps to Enhance the GERD Study

1. Update evapotranspiration of crops and free surface evaporation to be sensitive to temperature. If data is available, temperature effects on crop yields need to be added.

2. Population and GDP scenarios need to be aligned to IPCC CMIP5 RCP 8.5's corresponding assumptions.

3. Incorporate scenarios for Egyptian reactions to dropping water levels need to be incorporated. The Egyptians will have to make decisions about which sectors of their economy will suffer and which sectors to develop. For example, introducing an increase in groundwater pumping could offset Egyptian losses.

4. Several climate scenarios from CMIP5 could be added to obtain a sense of variations in wet and dry seasons.

5. Historic runoff data from GRDC needs to be used to remove bias from GCM projections. Trends can then be established by comparison of GCMs and historic data.

6. The search for more accurate water demand, and bathymetric data for Sudan needs to continue.

7. An investigation for data in the FPUs for Uganda, Djibouti, and Eritrea needs to begin.

8. The agricultural portion of WWAM needs to be calibrated to reflect food production for all 17 commodities. A food effectiveness factor needs to be added for the raw outputs of the model.

5.2. Long Term Developments

1. Development of methods to calculate the inputs to WWAM independent of the original WSM and IMPACT sets originally provided is needed. An automated link between data sources such as AQUASTAT and FAO Food Production would make it much easier to calibrate the model for the entire world as new data sets are generated in the future.

2. Reprogram WWAM so that all input is consolidated in a single storage location such as a relational database or XML file so that data configurations are easier to handle. Currently, there is no distinct separation between the algorithms and the data.

3. Reprogram WWAM to have a single set of consistent units. Also eliminate all numerically typed constants.

4. Reprogram WWAM to tightly couple WSM and IMPACT with the same time step. Currently WWAM iterates between running WSM and IMPACT.

5. Continue development of WWAM to include better conversion of food production to actual delivery of food to the population and translating this to caloric intake and nutritional health of the populations involved.

6. Continue development of WWAM to include agent based decisions which change the water policy inputs that are currently set as constants. These decisions could be based on water shortage histories.

6. CONCLUSION

WAMM has been demonstrated to have the capability to answer important policy questions concerning the fill rate for the Grand Ethiopian Renaissance Dam. The scenarios developed use input data which inevitably lead to loss of Egyptian water storage in Lake Nasser. The current results assume a passive Egyptian response which is not expected in the real world, but helps illustrate the necessity of Egyptian action to meet its future water needs.

This Page is Intentionally Left Blank

7. REFERENCES

Abdelsalam, N.M., M.M. Abdelaziz, A.F. Zobaa, M.S. Aziz, 2008. "Toshka Project Electrical Power Demand (Mubarak Pump Station)," *Twelfth International Water Technology Conference (IWTC12)*, Alexandria, Egypt.

Aich, V., S. Liersch, T. Vetter, S. Huang, J Tecklenburg, P. Hoffmann, H. Koch, S. Fournet, V. Krysanova, E. N. Muller, F. F. Hattermann, 2014. "Comparing impacts of climate change on streamflow in four large African river basins." *Hydrology and Earth Systems Sciences* 18:1305-1321.

Alkama, R., L. Marchland, B. Decharme, 2013. "Detection of global runoff changes: results from observations and CMIP5 experiments." *Hydrology and Earth Systems Sciences Discussions* 10: 2117-2140.

Backus, George et. al.,2012. "Risk Assessment of Climate Systems for National Security" *Sandia National Laboratories Technical Report* SAND2012-10554 (October): 66-81

Backus, George A., Michael L. Bernard, Stephen J. Verzi, Asmeret B. Bier, Matthew R. Glickman, 2010. "Foundations to the unified psycho-cognitive engine." *Sandia National Laboratories Technical Report* SAND2010-6974 (October).

Bernard, Michael L., George A. Backus, Asmeret Bier Naugle, Robert F. Jeffers, and Regan W. Damron, 2016. "Anticipating the Potential Range of Behaviors for Individuals Interacting Within Societies." In *Modeling Sociocultural Influences on Decision Making: Understanding Conflict, Enabling Stability,* edited by Joseph V. Cohn, Sae Schatz, Hannah Freeman, and David J.Y. Combs, In Press. CRC Press, October, 2016.

Beyene, Tazebe, Dennis P. Lettenmaier, Pavel Kabat, 2010. "Hydrologic impacts of climate change on the Nile River Basin: implications of the 2007 IPCC scenarios." *Climate Change* 100:433-461.

Cai, X.M., Rosegrant, M.W., 2002. "Global water demand and supply projections part -1. A modeling approach," *Water International* 27, no. 2 (June): 159-169

Center for International Earth Science Information Network (CIESIN), 2002. *Country-level Population and Downscaled Projections based on the B2 Scenario, 1990-2100,* [digital version]. Palisades, NY: CIESIN, Columbia University. Available at http://www.ciesin.columbia.edu/datasets/downscaled. (Accessed 9/23/2014)

Center for International Earth Science Information Network (CIESIN), 2002. *Country-level GDP and Downscaled Projections based on the A1, A2, B1, and B2 Marker Scenarios, 1990-2100,* [digital version]. Palisades, NY: CIESIN, Columbia University. Available at http://www.ciesin.columbia.edu/datasets/downscaled. (Accessed 9/23/2014)

Crétaux, J.F. , W. Jelinski , S. Calmant , A. Kouraev , V. Vuglinski , M. Bergé Nguyen , M-C. Gennero , F. Nino, R. Abarca Del Rio , A. Cazenave , P. Maisongrande, 2011. "SOLS: A Lake database to monitor in Near Real Time water level and storage variations from remote sensing data," *Advances in Space Research* 47, no. 9 (May): 1497-1507 http://www.legos.obs-mip.fr/en/soa/hydrologie/hydroweb/

Conway, D. and M. Hulme, 1993. "Recent fluctuations in precipitation and runoff over the Nile sub-basins and their impact on main Nile discharge." *Climate Change* 25:127-151.

Donia, Noha, 2013. "Aswan High Dam Reservoir management system," *Journal of Hydroinformatics* 15, vol, 4 (May): 1491-1510.

Food and Agriculture Organization of the United Nations (FAO), 2004. AQUASTAT. Database, FAO. www.fao.org (reference from Yang et. al. 2007 Table 1)

Elshamy, M. E., I. A. Seierstad, A. Sorteberg, 2009, "Impacts of climate change on Blue Nile flows using bias-corrected GCM scenarios." *Hydrology and Earth System Sciences* 13:551-565.

Hossain, Md. S., A. El-Shafie, 2014. "Performance analysis of artificial bee colony (ABC) algorithm in optimizing release policy of Aswan High Dam," *Neural Computations and Applications* 24: 1199-1206.

Hwang, Syewoon, Wendy D. Graham, 2014. "Assessment of Alternative Methods for Statistically Downscaling Daily GCM Precipitation Outputs to Simulate Regional Streamflow." *Journal of the American Water Resources Association* (JAWRA) 50(4): 1010-1032.

Intergovernmental Panel on Climate Change (IPCC), 2007. *Contribution of Working Groups I, II, and III to the Fourth Assessment Report of the Intergovernmental Panel on Climate Change*, Geneva, Switzerland

King, Andrew M. 2013. "An Assessment of Reservoir Filling Policies under a Changing Climate for Ethiopia's Grand Renaissance Dam," Master's thesis, Drexel University.

Longuevergne, L., C. R. Wilson, B.R. Scanlon, J.F. Crétaux, 2013. "GRACE water storage estimates for the Middle East and other regions with significant reservoir and lake storage," *Hydrology and Earth System Sciences* 17:4817-4830.

Mohamed, Yasir, H.H.G Savenije, 2014. "Impact of climate variability on the hydrology of the Sudd wetland: signals derived from long term (1900-2000) water balance computations," *Wetlands Ecological Management* 22:191-198.

Muala, Eric, Yasir A. Mohamed, Zheng Duan, and Pieter van der Zaag, 2014. "Estimation of Reservoir Discharges from Lake Nasser and Rosaries Reservoir in the Nile Basin Using Satellite Altimetry and Imagery Data," *Remote Sensing* 6 (August): 7522-7545

Rosegrant, Mark W., Claudia Ringler, Siwa Msangi, Timothy Susler, Tingju Zhu, Sarah Cline, 2008. "International Model for Policy Analysis of Agricultural Commodities and Trade (IMPACT): Model Description," *International Food Policy Research Institute Report*, Washington, D.C., June.

Sayed, M. A. A., 2004. "Impacts of climate change on the Nile Flows." PhD Thesis. Faculty of Engineering, Ain Shams University. Cairo, Egypt.

Strzepek, K.M., David N. Yates, 2000. "Responses and Thresholds of the Egyptian Economy to Climate Change Impacts on the Water Resources of the Nile River," *Climate Change* 46: 339-356.

Sutcliffe, J. V., Y. P. Parks, 1999. *The Hydrology of the Nile*, Oxfordshire, UK: The International Association of Hydrological Sciences.

Taylor, Karl E., Ronald J. Stouffer, Gerald A. Meehl, 2012. "An Overview of CMIP5 and the Experiment Design," *American Meteorological Society* April: 485-498.

United Nations, Department of Economic and Social Affairs, Population Division, 2011. *World Population Prospects: The 2010 Revision, Volume I: Comprehensive Tables.*

World Bank (2014) Population Data
http://data.worldbank.org/indicator/SP.POP.TOTL (Accessed 9/23/2014)

World Bank (2012) Nile River Basin Map. Printing and Multimedia, General Services Department, the World Bank Group.

Yang, H., L. Wang, A. J. B. Zehnder, 2007. "Water scarcity and food trade in the Southern and Eastern Mediterranean countries," *Food Policy* 32: 585-605.

DISTRIBUTION

External Distribution

Electronic copies to:

Peter Engelke, Atlantic Council at pengelke@atlanticcouncil.org
Ximing Cai, University of Illinois at xmcai@illinois.edu

Internal Distribution

1	MS0421	Tom Nelson	00159
1	MS0421	Howard Passell	00159
1	MS0751	Barry Roberts	06912
1	MS1137	Vincent Tidwell	06926
1	MS1138	Stephanie Kuzio	06926
1	MS1138	Daniel Villa	06926
1	MS0899	Technical Library	9536 (electronic copy)


Sandia National Laboratories